



La Région
Auvergne-Rhône-Alpes

ABSTRACTS BOOK

ELyT workshop 2025

**International Research Network
IRN CNRS “ELyT Global”**

Engineering and science Lyon Tohoku



February 19th – 21st, 2025 – Lyon / Annecy, France



ELyT workshop 2025

Februray 19th - 21st, 2025 - France

Program

Wednesday, February 19th

INSA Lyon (INL amphitheater)

8:30	9:00	Welcome coffee and registration
9:00	9:40	Opening of the workshop
9:40	10:20	Keynote 1
10:20	11:00	Keynote 2
11:00	11:20	Break
11:20	12:00	Keynote 3
12:00	12:30	JSPS presentation

12:30	13:50	Lunch and poster session
-------	-------	--------------------------

13:50	14:00	Tribute to Georges Boulon
14:00	14:40	Keynote 4
14:40	15:20	Keynote 5
15:20	16:00	Keynote 6
16:00	17:00	Coffee break and poster session
17:00	18:25	Session 1

		Dinner (on your own)
--	--	----------------------

Thursday, February 20th

Anecny (Le Pré du Lac - Saint-Jorioz)

7:40		Bus departure from INSA Lyon to Anecny
		Bus trip to Anecny
10:40	12:15	Session 2

12:15	13:45	Lunch
-------	-------	-------

13:45	15:50	Session 3
15:50	16:35	Coffee break and free discussion
16:35	18:20	Session 4

		Dinner
--	--	--------

Friday, February 21st

Anecny (Le Pré du Lac - Saint-Jorioz)

9:00	9:40	Keynote 7
9:40	10:40	Session 5
10:40	11:10	Break
11:10	12:15	Session 6
12:15	12:30	Closure of the workshop

12:30	14:00	Lunch
-------	-------	-------

		Social activity: PACCARD Museum (bell museum visit + workshops guided tour)
14:30	16:15	
16:30	18:30	Bus trip to Lyon

		Dinner (on your own)
--	--	----------------------

Wednesday, February 19th

INSA Lyon (INL amphitheater)

8:30	9:00	Welcome coffee and registration
9:00	9:40	Opening of the workshop
9:40	10:20	Keynote: Fuel and Structural Materials analysis in Nuclear Power Plants Jonathan Quibel (ASNR)
10:20	11:00	Keynote: Electro-mechanical degradation in solid state batteries probed by multiple characterisation techniques Claire Villevieille (INP Grenoble)
11:00	11:20	Short break
11:20	12:00	Keynote: An R&D strategy dedicated to fostering a mechanical industry that is more autonomous, optimistic, and sustainable Fabien Lefebvre (CETIM)
12:00	12:30	JSPS presentation Toshiyuki Takagi
12:30	13:50	Lunch and poster session
13:50	14:00	Tribute to Georges Boulon, by Amina Bensalah-Ledoux (UCB Lyon 1)
14:00	14:40	Keynote: Principles and applications of ultrasonic transducers Guy Feuillard (INSA Centre Val de Loire)
14:40	15:20	Keynote: 3D local magnetoresistive probe for magnetic imaging diagnostics Aurélie Solignac (CEA)
15:20	16:00	Keynote: Controlling friction in rubber materials through advanced strain measurement and tread design Takeshi Yamaguchi (TU)
16:00	17:00	Coffee break and poster session
17:00	17:25	Towards the Control of Protein Mass Transfer via Ultrasound and Macro-porous Membranes Atsuki Komiya (TU), Sophie Miralles (INSA Lyon) <i>et al.</i>
17:25	17:45	Monitoring Eukaryotic Cell Functions under Various Hypoxic Conditions with Microfluidic Based Oxygenators Jean-Paul Rieu <i>et al.</i> (UCBL)
17:45	18:05	Analysis of Guidewire Technique aiming for Reducing the Load on Vessels at the Internal Carotid Artery Bend Ayami Omiya <i>et al.</i> (TU)
18:05	18:25	EM Tracking of Catheter Louis Paquet <i>et al.</i> (INSA Lyon)

Thursday, February 20th

Annecy (Le Pré du Lac - Saint-Jorioz)

7:40		Bus departure from INSA Lyon to Annecy
		Bus trip to Annecy
10:40	11:05	Ion-doped polymer actuators : experiments and modeling Hidemasa Takana (TU), Joël Courbon (INSA Lyon) et al.
11:05	11:30	Application of Electromagnetic Non-Destructive Testing on Steel Bearing Components: SKF-ELyTMaX collaboration Bhaawan Gupta (SKF), Benjamin Ducharne (INSA Lyon) et al.
11:30	11:50	Incorporating TRIP/TWIP effects in duplex titanium alloys Kenta Yamanaka et al. (TU)
11:50	12:15	Electric Field Dependence of Parameters Related to the C Diffusivity in Steel and Improvement of Previous Analytical Model Ryuta Onozuka (TU), Takashi Tokumasu (TU) et al.
12:15	13:45	Lunch
13:45	14:05	Interfacial Thermal Resistance at Solid-Liquid Interfaces with Complex Morphologies: Evaluation and Interpretation via Molecular Dynamics Donatas Surblys et al. (TU)
14:05	14:25	Natural Rubber Foil-Based Elastocaloric Cooling using Bistable Actuation Carina Ludwig et al. (Karlsruhe Institute of Technology)
14:25	14:50	Heat transfer control for solid-state refrigeration using natural rubber Atsuki Komiya (TU), Gaël Sebald (ELyT MaX) et al.
14:50	15:10	Organic LEDs Based on Bis(8-hydroxyquinoline) Zinc Derivatives Alexandra Apostoluk et al. (INSA Lyon)
15:10	15:30	Nanoscaled ferroelectric binary oxide thin film supercapacitors for flexible and ultrafast pulsed power electronics Bertrand Vilquin et al. (Centrale Lyon)
15:30	15:50	Oxidation and deoxidization process of semiconductors and metals Kazuhiko Endo et al. (TU)
15:50	16:35	Coffee break and free discussion
16:35	17:00	Fe-Al arc welding: predicting the formation of the intermetallic compound layer by finite elements method simulation Benjamin Leflon (TU), Sylvain Dancette (INSA Lyon) et al.
17:00	17:20	Metallization on Oxide Ceramics by Low Pressure Cold Spray and Its Deposition Mechanism Analyses Kazuhiro Ogawa et al. (TU)
17:20	17:40	Insights into Solid Lubrication Processes of DLC Films thanks to Analytical Tribology Julien Fontaine et al. (Centrale Lyon)
17:40	18:00	Multiscale Analysis of the Rubber/Ice Tribological interface Anderson Dalavale Kaiser Pinto et al. (Centrale Lyon)
18:00	18:20	Mechano-Chemically-activated Tribofilm Growth at Nanoscale Maria-Isabel de Barros Bouchet et al. (Centrale Lyon)

Friday, February 21st

Annecy (Le Pré du Lac - Saint-Jorioz)

9:00	9:40	Introduction of Integrated Flow Science and recent activities of the Institute of Fluid Science, IFS, Tohoku University Kaoru Maruta (TU)
9:40	10:00	Multi-scale study on cavitating flow with liquid-vapor phase change Shin-ichi Tsuda <i>et al.</i> (Kyushu University)
10:00	10:20	Solid particle impact on CO ₂ absorption among phytoplankton blooms Serge Simoëns <i>et al.</i> (Centrale Lyon)
10:20	10:40	Robust Multi-objective optimization schemes : applications for shape design of mechanical parts Frédéric Gillot <i>et al.</i> (Centrale Lyon)
10:40	11:10	Break
11:10	11:30	EBI Induced Ductility of Brittle 3D-Printed Short Fiber Reinforced PA Helmut Uchida <i>et al.</i> (Tokai University)
11:30	11:50	Sensor-Less Structural Health Monitoring using Semi-Active Controlled Piezoelectric Transducer Yushin Hara <i>et al.</i> (TU)
11:50	12:15	Last progress in magnetic NDT in the framework of the BENTO project Yves Armand Tene Deffo (TU), Tetsuya Uchimoto (TU) <i>et al.</i>
12:15	12:30	Closure of the workshop
12:30	14:00	Lunch
14:30	16:15	Social activity: PACCARD Museum (click on the logo to go to the website) (bell museum visit + workshops guided tour) 
16:30	18:30	Bus trip to Lyon

1st day – INSA Campus

INL amphitheater –
workshop location

GPS coordinate:
45°46'59.9"N
4°52'05.3"E

T1/T4 tramway
station “La Doua –
Gaston Berger”



Google map link :
<https://maps.app.goo.gl/cAnP2pSdECdwjBpu8>



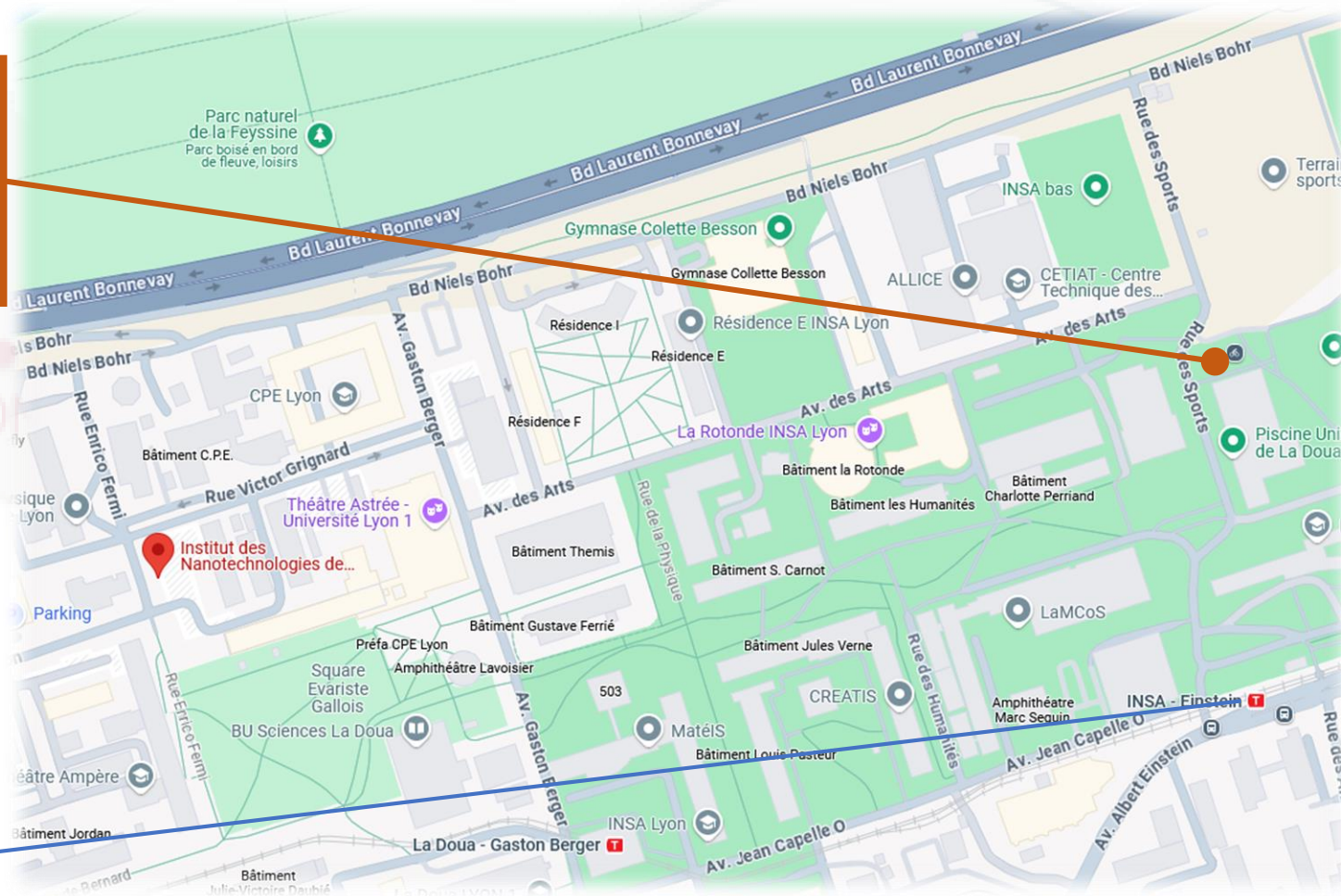
<https://www.google.fr/maps/>



2nd day – bus to Annecy

INSA gymnasium/
swimming pool
parking

GPS coordinate:
45°47'04.0"N
4°52'38.3"E



Google map link :
<https://maps.app.goo.gl/YEUcdZJFZ2mq64Di6>



T1 tramway station
“INSA – Einstein”

<https://www.google.fr/maps/>






**Wednesday,
February 19th**

Morning

Fuel and Structural materials analysis in Nuclear Power Plants

ELyT Global Nuclear Materials

	<p>Jonathan Quibel</p> <p>French Nuclear Safety and Radiation Protection Authority</p> <p>(ASNR)</p>		<p>Jean Desquines</p> <p>French Nuclear Safety and Radiation Protection Authority</p> <p>(ASNR)</p>
	<p>Séverine Guilbert</p> <p>French Nuclear Safety and Radiation Protection Authority</p> <p>(ASNR)</p>		

Abstract

In the nuclear industry, various materials are used such as composites, concretes, polymers and metals. The degradation of these materials is a major topic of interest for the French Nuclear Safety and Radiation Protection Authority (ASNR).

Safety evaluation relies on demonstrating the safety of a considered component under accidental loadings/transients. The strategy is to prove a safe behaviour of the reactor under penalizing transients and conditions to ensure that less demanding situations are inherently covered. Hence, to assess the resistance of the nuclear materials, our team generates experimental data and mechanisms understanding for modelling and simulation codes.

Since our laboratory does not have hot cells, we typically simulate irradiation conditions. This approach allows us to address a wide range of safety activities without relying







on hot cells, ultimately aiming to minimize the number of tests required on irradiated materials.

Structural materials of the primary loop in Pressurized Water Reactors (PWR), which is the second confinement barrier, must sustain a nominal temperature and pressure of 300°C and 155 bars in a corrosive environment for years. This leads to the study of ageing of nuclear materials to safely assess the Long-Term Operation of Nuclear Power Plants. In addition, to prevent design issue, Low Cycle Fatigue is evaluated using loadings and environments covering any possible thermal transient under the reactor operation. The phenomenon studied here is Environmentally Assisted Fatigue on stainless steels and nickel-based alloys. Hence, our laboratory is involved in different European programs such as INCEFA-SCALE and NUCOBAM dealing with these topics.

For fuel safety evaluations, the postulated accidents cover a wide range of situations. However, our laboratory mainly addresses Loss of Coolant Accident and transportation/dry storage studies. The fuel rods are constituted of piled fuel pellets inserted into 4 meters long zirconium alloy claddings. The laboratory has much more activity on fuel claddings, which is the first confinement barrier, rather than irradiated pellets studies. However, the development of mock-up irradiated pellets is addressed in the lab activities. Hence, our laboratory is involved in different international programs such as SCIP and QUENCH-ATF.

**Electro-mechanical degradation in solid state batteries
probed by multiple characterisation techniques**

**ELyT Global
Energy
Batteries and characterisations**

	<p>Claire Villevieille LEPMI – CNRS 1130 rue de la piscine 38402 Saint Martin d’Hères</p>		<p>Patrice Perrenot LEPMI – CNRS 1130 rue de la piscine 38402 Saint Martin d’Hères</p>
	<p>Oskar Thompson LEPMI – CNRS 1130 rue de la piscine 38402 Saint Martin d’Hères</p>		<p>Adrien Fauchier Magnan LEPMI – CNRS 1130 rue de la piscine 38402 Saint Martin d’Hères</p>
	<p>Lucas Trassart LEPMI – CNRS 1130 rue de la piscine 38402 Saint Martin d’Hères</p>		<p>Ove Korjus Institut Laue Langevin (ILL) Avenue des Martyrs 38000 Grenoble</p>

Abstract

All-solid-state batteries have been presented as the ideal solution to address i) the safety limitations of conventional Li-ion batteries by suppressing the flammable organic electrolytes and ii) the problem of insufficient energy densities if coupled to Li metal. To date, two types of solid Li-ion electrolytes have been mainly studied, namely, thiophosphate materials and ceramic-based materials. As they are easy to process and

they offer a high ionic conductivity in the range of 1-20 mS/cm, thiophosphate electrolytes such as e.g. thio-LISICONs and argyrodites are therefore regarded as suitable candidates to be used in lithium all-solid-state batteries.

Despite the progress in the development of superionic conductor, many aspects regarding their chemical and mechanical issues remain unsolved especially during electrochemical activities where the electrolyte is heavily decomposed. If the electrode engineering i.e. composite electrode (mixture of electroactive material, conductive agent and solid electrolyte) is under intense investigation, the role of the solid electrolyte used as separator is so far poorly studied. Quite often, the electrochemical fading mechanisms observed with ageing are solely ascribed to the conventional fading parameters (cycling, temperature, interfacial reaction, chemo-mechanical degradation), but it might be that most of those parameters are happening prior any electrochemical activities during the sintering process.

As an example, if the sintering (even cold sintering) is not properly performed, voids will appear in the solid electrolyte pellet, and during charge/discharge, the same voids could then evolve and propagate into cracks causing mechanical failure.

In this work, two different microstructure & morphological evolution will be monitored.

- The first one will focus on the relationship between the sintering parameters (time/pressure) of the thiophosphate materials and the pore network percolation¹
- The second one will be based on an in-depth operando investigation of the microstructure evolution of the solid electrolyte and of the composite electrode²

Operando XRD-CT, XCT and FIB-SEM were selected as techniques of choice to establish the correlation between electrochemistry, microstructure, morphology, and electrochemical fading. The results obtained here should serve as a preliminary basis to develop better solid-state batteries.

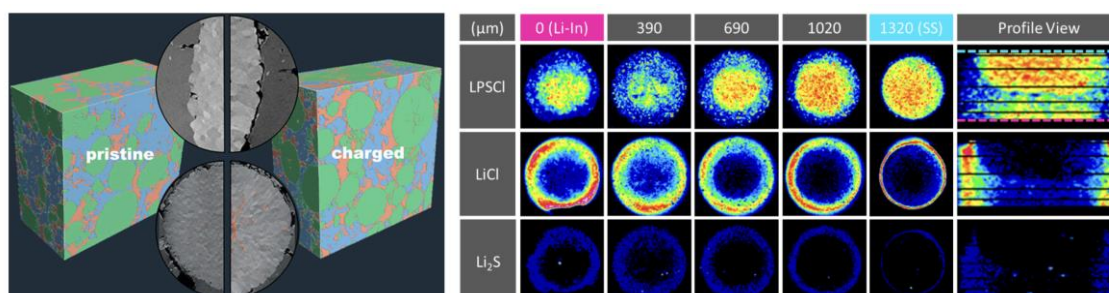



Figure 1. Left) Microstructure of LSPCLi/NMC622 composite electrode investigated by operando FIB-SEM; Right) XRD-CT investigation (performed at ID15a, ESRF) of a half-cell LPSCLi/Li-In aged for 20 cycles.

1. Perrenot P, Fauchier-Magnan A, Mirolo M, Lecarme L, Jouneau P-H, Boulineau A, *et al.* Room-Temperature Sintering of Amorphous Thiophosphate Solid Electrolyte (Li_3PS_4): Coupling Morphological Evolution to Electrochemical Properties. *Advanced Functional Materials* 2024, **34**(2): 2310739.
2. Perrenot P, Bayle-Guillemaud P, Villevieille C. Composite Electrode ($\text{LiNi}_{0.6}\text{Mn}_{0.2}\text{Co}_{0.2}\text{O}_2$) Engineering for Thiophosphate Solid-State Batteries: Morphological Evolution and Electrochemical Properties. *ACS Energy Letters* 2023, **8**(11): 4957-4965.

**An R&D strategy dedicated to fostering
a mechanical industry that is more
autonomous, optimistic, and sustainable.**

	<p>Dr. -Ing Fabien Lefebvre</p> <p>Cetim Scientific Advisor</p> <p>Cetim</p>		
--	---	--	--

Abstract

Cetim, the Technical Center for Mechanical Industries, was established in 1965 at the request of mechanical industry companies to provide them with the means and skills necessary to improve their competitiveness, participate in standardization, establish a relationship between scientific and industrial research, promote technical progress, provide assistance to improve performance, and ensure quality. Cetim is now focusing on technological and organizational research programs in an increasingly open European and international context.

Cetim supports companies, particularly in industrial sectors, to improve their competitiveness, performance, and sustainability. In terms of R&D, a new strategy has been implemented for the years 2024-2027 through a structured 'funnel' approach. This has resulted in a section dedicated to R&D shifts, requiring acceleration of an R&D dynamic, and a section dedicated to fundamental skills for the mechanical engineering sector such as design, sizing, optimization, and manufacturing, then finally control, monitoring, and validation. Five shifts have been highlighted: decarbonization and water economy, circularity and sustainable materials, digital transformation, energy systems, and finally low-carbon mobility. Strategic projects have been implemented to support this R&D roadmap as HYMEET, CEDRE or E-MOBILITY program.

Fostering Global Research Connections: Activities and Opportunities at the JSPS Strasbourg Office

<https://jsps-strasbourg.com/>

	<p>Prof. Toshiyuki TAKAGI</p> <p>JSPS Strasbourg Office</p> <p>Director</p>	<p>Ms. Tomoko YAMAGUCHI</p> <p>JSPS Strasbourg Office</p> <p>Deputy-Director</p>	<p>Mr. Kota SAKURAI</p> <p>JSPS Strasbourg Office</p> <p>International Program Associate</p>
---	--	---	---

Abstract

The Japan Society for the Promotion of Science (JSPS), established in 1932, is Japan’s leading funding agency dedicated to advancing academic research across all fields, including humanities, social sciences, and natural sciences. Unlike mission-oriented, top-down approaches, JSPS employs a bottom-up approach, supporting researchers’ curiosity-driven ideas and enabling independent research activities. Through its global network of ten overseas offices, including the Strasbourg Office established in 2001, JSPS promotes international academic collaboration and researcher exchange.

This lecture introduces the key activities of the JSPS Strasbourg Office, which promotes JSPS international programs, including individual fellowships, bilateral research projects, and multilateral collaborations. Key programs include postdoctoral and invitational fellowships, the Bridge Fellowship for alumni, and bilateral partnerships with institutions such as Inserm, the French National Institute of Health and Medical Research, ANR, the French National Research Agency, and the French Ministries of Europe and Foreign Affairs (MEAE) and Higher Education and Research (MESR). JSPS also engages in the management of the Summer Program and Frontiers of Science in collaboration with CNRS, the French National Centre for Scientific Research. Furthermore, the office organizes academic forums and networking events, fostering connections among researchers and facilitating the global exchange of knowledge. Through these efforts, the JSPS Strasbourg Office serves as a vital bridge between European and Japanese researchers, contributing to the advancement of global scientific networks.



**Wednesday,
February 19th**

Poster sessions

Mass and thermal transfers in case of flat plate impacting multijets.

ELyT Global

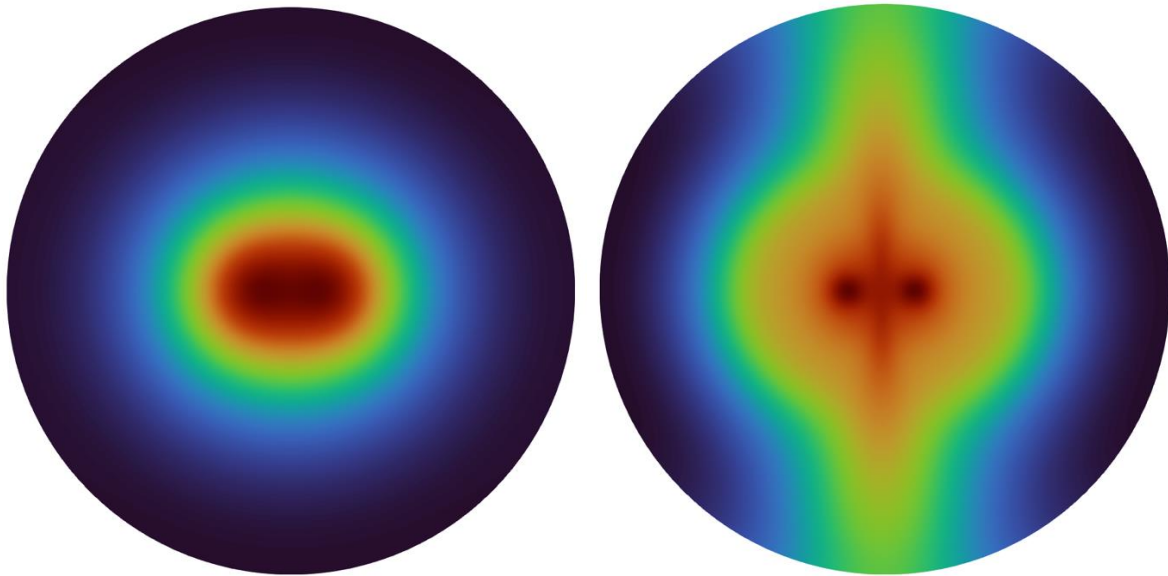
**Theme Thermal and Mass tranfers,
Scientific topic thermal and Mass transfers,
impacting jets, chemical reaction.**

	<p>Dr S. Simoëns, CNRS Research Director</p> <p>LMFA, ECL, INSA, UCB Lyon I, UMR CNRS 5509</p>		<p>Pr. I. Vinkovic, Th. Juhan, Doctorant</p> <p>LMFA, ECL, INSA, UCB Lyon I, UMR CNRS 5509</p>
--	---	---	--

Abstract

Heterogeneous photocatalysis offers the promise of powering chemical processes with highly abundant and renewable solar energy. In particular, photocatalytic conversion of molecules such as H₂O or CO₂ into valuable fuels has been the focus of an ever-increasing research effort for the past few decades. While significant progress has been made in photocatalyst design, there are still significant knowledge gaps in the understanding and the optimization of catalyst active sites. In this work we hypothesized a situation with a catalic plate at the bottom of an open domain as for example studied by ([1], Matera et al.). The project aims to understand chemical product injection on such a plate with potential plate heating and search also to characterize a model catalytic reaction.

In this context, the aim of our team is to perform fluid dynamics numerical simulations of product injections via top injection as in [2]. We propose different geometries and configurations in the spirit of Materas et al. ([1]) but this kind of configuration could be applied in case of cooling optimization of a single heating plate with fresh incoming gas flow (square, circular or conical injectors). This is studied using the opensource code OpenFoam. To answer issues on flow-dynamics and species transport impact on the efficiency of the system, the influence of temperature on the flow is accounted for within the simulations. Validation is done via classical chemical reactions.



Reactant concentration on a photocatalytic cell. Injection from two jets at different Reynolds numbers $Re=50$ (left), $Re=300$ (right). Blue (red) regions correspond to low (high) reactant concentrations.

[1] S. Matera and K. Reuter, *Journal of Catalysis*, vol. 295, 2012.






[2] T. Juhan, I. Vinkovic, S. Simoëns Flow dynamics, heat and mass transfer of laminar, round twin-jet impinging a uniformly heated flat plate, [International Journal of Heat and Mass Transfer](#)

[Volume 236, Part 1](#), January , 126187, 2025

**Hemodynamic and biomarkers in case of aorta blood circulation:
different weakening situations.**

ELyT Global

**Theme : Health, hemodynamic
Scientific topic : hemodynamics, blood flow,
surgery, fistula, stent deposition bank.**

	<p>Dr S. Simoëns, CNRS Research Director</p> <p>LMFA, ECL, INSA, UCB Lyon I, UMR CNRS 5509</p>	   	<p>Dr. M. El Hajem, Dr. P. Kulisa Pr. I. Vinkovic Dr A. Moravia R. Courteau, stage,</p> <p>LMFA, ECL, INSA, UCB Lyon I, UMR CNRS 5259</p> <p>Pr. Ben Bousaid,</p> <p>LAMCOS, INSA, UMR CNRS 5509</p>
---	---	---	--

Abstract

We deal with individualized medicine. For example, we are interested in FAV (Fistula Arterio Vena). The construction of the FAV requires connecting the arteries to the superficial blood vein, conditioned by dialysis conditions [1]. This requires an anastomosis shunt of diameter (D_a) and angle (θ) to be defined according to a specific patient; it will induce, a posteriori, a new intra-vascular hemodynamics (figure 1).

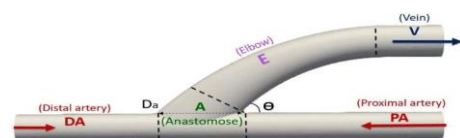


Figure 1 : Representation of an AVF with its different characteristic quantities.

This affects the expansion and re-modeling of the vein which is no longer under control at the end of the operation. We have still built a computational and experimental platform to help surgeons better control the individual anastomosis planning process, to reduce patient pain and medical costs associated with post-operative complications. Most of the patient-specific information comes from medical imaging in the form of MRIs and scans [2].

For pre-surgical assistance, there are at least two possible techniques: experimental reproduction of the In Vitro blood system associated with advanced laser metrologies and high performance computational mechanics (fluid dynamics and structure coupling) both reproducing, until now, only partially realistic In Vivo Arterio-Vena blood system. To our knowledge, few experimental setups have obtained local and instantaneous velocity measurements (via Particle Image Velocimetry (PIV) (Tracking)) using a bio-faithful reproduction of the vein, with consistent material properties of the tissues and realistic patient-specific blood flow subjected to the cardiac cycle. Literature exists for Arterio-Vena experiments with PIV measurements but for rigid walls [3], which could not reproduce realistic shears and deformations at the vein walls level. Few works have considered the elastic properties of arteries unlike that of M. Menut [4]. In recent work, a geometrically bio-faithful phantom in transparent and elastic polymer has recently been used to carry out such original PIV measurements [5]. Realistic blood reproduction (considering non-Newtonian properties), respecting the very fine requirements of hemorheology (6) is very rarely used for in vitro measurements [5] even for rigid veins reproduction. Another inspection tool is computational fluid mechanics for In Vivo Arterio-Vena geometries. Little or no work has shown such flow simulations considering both elasticity of the Arterio-Vena material and rheological blood properties. Recent work by Lee et al. [7] is, for example only related to Newtonian fluid.

The very recent @NEDA project (PhD A. Moravia, PhD WY. Pan [5,9]) uses an experimental device for the inspection of flow modifications **during the placement of a stent inside a full-scale artero-vein system under cardiac blood cycle**, considering vessel elasticity [4] and hemorheology with Varant et al. (6) recommendations. Therefore, the results obtained ([5]) under these conditions consider the PIV / Wall displacement coupling measurements (VWD). A joint digital model taking into account the fluid/structure issues has also been developed [9]. These results provide additional information to clinicians for surgical planning.

In the present future we have the same objective of helping surgical planning for stenting intervention due to atheroma plagues in any kind of artera geometry.

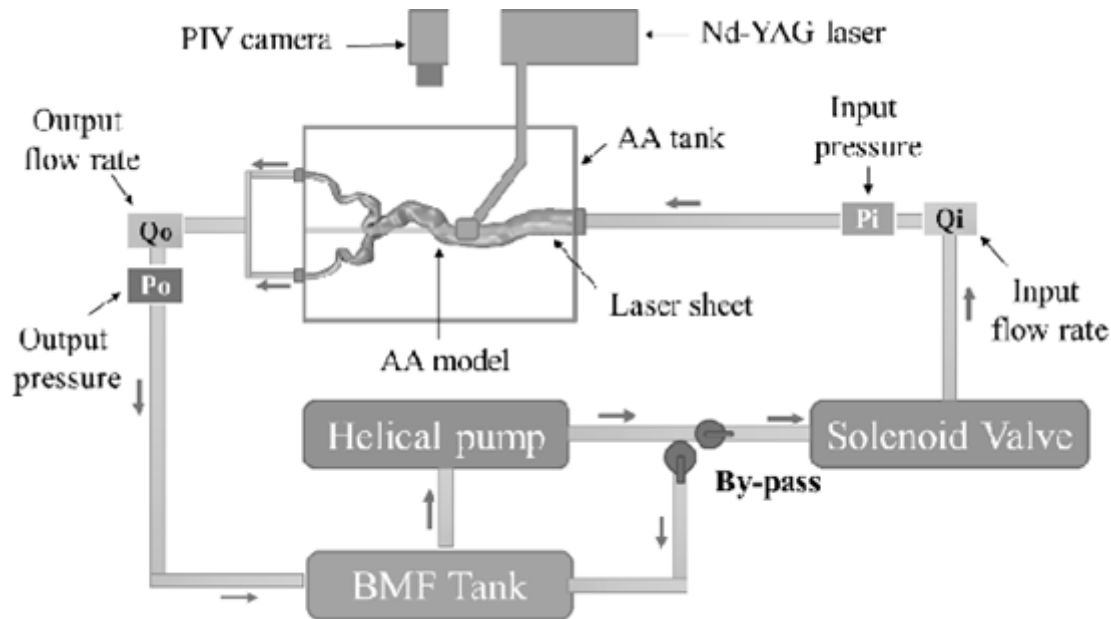


Figure 2: Top view of the experimental set-up. Arrows describe flow direction in the circuit.

- [1] B. S. Dixon, "Why don't fistulas mature ?" *Kidney international* 70.8 (2006): 1413-1422.
- [2] Badero, Olurotimi J., et al. "Frequency of swing-segment stenosis in referred dialysis patients with angiographically documented lesions." *American journal of kidney diseases* 51.1 (2008): 93-98.
- [3] Canaud, Bernard, et al. "Vascular Access Management for Haemodialysis: A Value-Based Approach from NephroCare Experience." *Vascular Access Surgery-Tips and Tricks*. IntechOpen, 2019.
- [4] M. Menut, L. Bousset, X. Escriva, B. Bou-Saïd, H. Walter-Le-Berre, Y. Marchesse, A. Million, N. Della Schiava, P. Lermusiaux, J. Tichy 'Comparison between a generalized Newtonian model and a network-type multiscale model for hemodynamic behavior in the aortic arch: Validation with 4D MRI data for a case study' *Journal of Biomechanics* 73 (2018) 119–126.
- [5] A Moravia, S Simoëns, M El Hajem, B Bou-Saïd, P Kulisa, Nellie Della-Schiava, Patrick Lermusiaux, [In vitro flow study in a compliant abdominal aorta phantom with a non-Newtonian blood-mimicking fluid](#), *Journal of Biomechanics* 130, 110899, 2022.
- [6] J. Ashkan, et al. "Analysis of blood flow characteristics in a model of a mature side to side arteriovenous fistula." *Artificial Organs* 41.11 (2017): E251-E262.
- [7] Lee, Sang-Wook, Luca Antiga, and David A. Steinman. "Correlations among indicators of disturbed flow at the normal carotid bifurcation." *Journal of biomechanical engineering* 131.6 (2009).
- [8] W Pan, P Kulisa, B Bou-Saïd, M El Hajem, S Simoëns, M Sigovan, [A proposal of risk indicators for pathological development from hemodynamic simulation: application to aortic dissection](#), *Journal of Cardiology and Cardiovascular Medicine* 8 (1), 029-038, 2023.

Acknowledgement : the present work is done with the help of the Carnot project Mimimed and the AURA Region program @NEDA.

MOREOVER project: Design of an EIS-based sensor for non-invasive
in-field corrosion monitoring

ELyT Global Energy Surfaces and interfaces

	<p><u>H. Abe</u>¹ Y. Watanabe^{1,2}</p>		<p><u>B. Ter-Ovanesian</u>³ N. Mary³ B. Normand³ <u>Z. Dong</u>^{2,3}</p>
---	--	--	--

Affiliation

¹ Graduate School of Engineering, Tohoku University, 6-6-01-2 Aoba, Aramaki, Aoba-Ku, Sendai, Japan

² ElyTMax UMI 3757, CNRS–Université de Lyon–Tohoku University, International Joint Unit, Sendai, Japan

³ INSA-Lyon, UCBL, UMR CNRS 5510 MATEIS, 69621 Villeurbanne Cedex, France

Abstract

1. Background

Nuclear power constitutes a significant component of both the French and Japanese energy source combination. Its ongoing operation and expansion are essential for realizing decarbonized energy goals. Nevertheless, effective management of nuclear waste remains a crucial factor influencing public acceptance and perception. The French Nuclear Safety Authority (ASN) classifies nuclear waste into two categories based on their radioactivity levels and lifespan: "short-lived" and "long-lived". "Short-lived" waste originates from activities such as the operation, maintenance, and decommissioning of nuclear power plants, including items like filters, used components, tools, and debris. On the other hand, "long-lived" waste primarily results from the processing of spent nuclear fuel. Geological disposal is internationally recognized as the benchmark solution for managing the most hazardous, long-lived radioactive waste.

The objective of a geological repository is to preserve both humanity and the environment from the effects of radioactive waste by containing radioactivity for up to several hundred thousand years. Most repository systems rely on multiple natural and/or artificial barriers to prevent the migration of radionuclides into the biosphere. Regardless of the chosen approach, extended corrosion period can occur on the overpack material (such as copper or non-alloyed steel) under specific environmental conditions. However, limited knowledge exists regarding the long-term

behavior of these materials when exposed to such environments that may undergo changes over expanded periods.

Since corrosion tests at the lab typically occur over short durations relative to the repository's timescale, mechanistically based modeling of corrosion product composition, formation mechanisms, and growth rates is necessary to forecast long-term behavior accurately. To propose consistent model, initial data acquisition is crucial. In this regard, archaeological artifacts serve as valuable resources, providing a database for validation and detailed investigation to validate the model. In this study in collaboration between INSA Lyon, Tohoku university and the National Research Institute for Cultural Properties in Nara, one approach involves conducting descriptive and quantitative analyses on samples of copper or iron alloys, referred to as archaeological analogs, which have experienced corrosion during burial for approximately 1,000 years. Nevertheless, legal regulations governing the protection of cultural heritage allow for chemical and physical characterization of excavated cultural objects using non-destructive techniques that preserve their value. Techniques such as X-ray diffraction, Raman spectroscopy, and visible light spectroscopy prove effective in detailing the complex chemical, physical, and morphological properties of corrosion product layers. These analyses will help identify the composition, thickness, and distribution of these layers during burial and elucidate the corrosion history of the samples. Complementary, the indirect electrolysis method will be used by developing an AC impedance measurement sensor with solid-state contacts. This method is prone not to damage the substrate and evaluate the oxidized material's corrosion rate [1].

Based on the collected results, the corrosion kinetics of the samples will be determined and implemented for developing models that predict the oxidation lifespan of the storage materials.

2. First Results

The first task of this study seeks to develop a non-destructive and immersion-free sensor utilizing electrochemical impedance spectroscopy (EIS), intended to offer detailed electrochemical insights into systems while being suitable for artifact measurement. The proposed sensor comprises two transparent 3D-printed cells connected to a potentiostat. One cell features a 99.99% platinum foil counter electrode and a low-profile Ag/AgCl reference electrode, while the other features a platinum foil working electrode. Both cells are filled with solid electrolyte using 0.1 M Na₂SO₄ gelled with 3% w-v agar and are positioned side by side on the surface under investigation. In preliminary tests, this EIS-based sensor was applied to various substrates, and its results were compared with conventional measurements to validate its accuracy. Special attention was paid to the sensor's response in relation to the measured impedance signal. When necessary, data processing was conducted to subtract the sensor impedance. The corrected results closely aligned with conventional measurements, with the modulus approximately doubled as the two-cell sensor measures the interface twice. This proposed "non-invasive" sensor has demonstrated its ability to consistently and accurately generate high-quality EIS spectra from laboratory samples. Given its distinctive non-invasive nature and adaptability, it seems potentially adapted to analyse archaeological artifacts.

[1] H. Kihira, S. Ito, T. Murata, *Corrosion* 1989, 45, 347.

Solid-state refrigeration based on natural rubber: Design and performances of two single stage elastocaloric cooling devices and analytical modelling

ELyT Global Theme: Energy Scientific topic: Materials and Structures Design

				
Marianne SION ^{a,b,c}	Atsuki KOMIYA ^{a,b}	Gaël SEBALD ^a	Shihe XIN ^c	Gildas COATIVY ^d

^a ELyTMaX IRL 3757, CNRS, Univ. Lyon, INSA Lyon, Centrale Lyon, Université Claude Bernard Lyon 1, Tohoku University, Sendai, Japan

^b Institute of Fluid Science, Tohoku University, Sendai, Japan

^c CETHIL UMR5008, F-69621, INSA-Lyon, CNRS, Université Claude Bernard Lyon 1, Villeurbanne, France

^d INSA Lyon, LGEF, UR682, Villeurbanne, France

Abstract

In the frame of solid-state cooling using caloric materials, the goal of this work is to develop an experimental proof of concept for an elastocaloric cooling system in a single stage configuration, based on natural rubber. The developed device consists of a natural rubber film, that is cyclically stretched and put in contact with hot and cold heat exchangers in a four-step process. During the 1st step, the NR film is stretched to an elongation of 6 (Fig. 1a). This causes a decrease in entropy throughout the material in isothermal condition, which translates in adiabatic condition in an increase of its temperature. In the second step, the Hot Heat Exchanger (HHEX) is being put in contact with the NR, in order to transfer the heat from the NR to the HHEX. At the third step, the HHEX is withdrawn from the contact after an adaptable contact time, then the NR film is unstretched to an elongation of 4, leading to a decrease in temperature because of the entropy increase in the material. The final step is to put the Cold Heat Exchanger (CHEX) in contact with the NR for a determined contact time to transfer heat from the CHEX to the NR and then the contact is withdrawn. After that, the 4- steps of the cycles are repeated, leading to a temperature span between both HHEX and CHEX. Further explanations about this experimental setup had been given in our previous work [1].

The performances of the experimental setup have been tested and had shown interesting and promising results, with temperature span up to 1.9°C and 0.4 W. We defined then the ultimate cooling power, defined as the cooling power when all the entropy variation induced by the elongation change translates into heat taken from the cold heat exchanger at every cycle. It was then compared to the actual measured cooling power. It was observed that for thinner samples,

the cooling power could reach up to 60% of the ultimate cooling power. Several other compositions were then tested, both tailored and commercial grades of natural rubber. It was observed that the composition do not impact significantly on the performances.

Another device combining the stretching step and the heat exchange step was then developed and tested in an attempt of device simplification (reduction of the number of actuators). It was observed slightly lower performances probably due to higher thermal losses and degraded thermodynamic cycle.

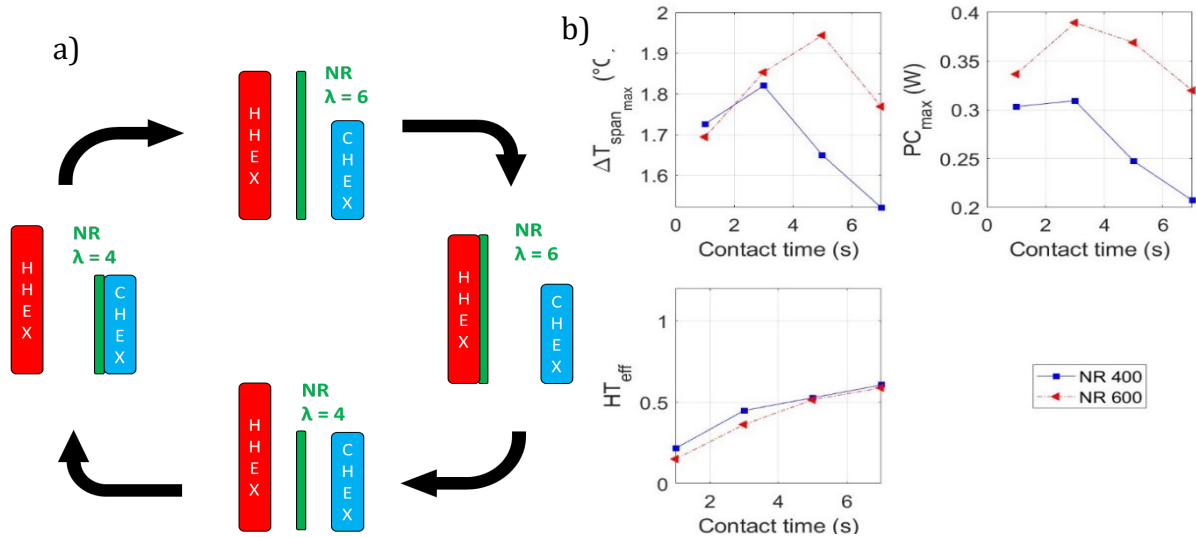


Fig. 1 (a) Schematic of the four-step cycle, (b) Performances of the experimental setup for NR 400 and NR 600; Temperature span, Cooling Power, Heat Transfer effectiveness

In an attempt to understand the solid-solid heat transfer dependence on the operating conditions, an 1D analytical modelling was developed. It consisted of solving the heat conduction equation at each step of the process, and simulating the thermal losses, both by convection and those associated with the heat exchangers imperfect thermal insulation. It was observed that thermal losses had to be set at a high value to catch the experimental data. Nonetheless, the model showed that the absolute cooling power depends weakly on the thickness of the natural rubber. Finally, after simplification of the model, it was determined the heat exchange time constant between the natural rubber and the heat exchangers. It was revealed two limit cases. For small thickness, the heat transfer is limited by the thermal resistance at the interface, and the time constant varies linearly with the thickness. For high thickness, it is limited by thermal diffusion within the natural rubber film and leads to a quadratic increase with the thickness, inducing a loss of performance. Interestingly, the threshold thickness depends on materials parameters only. It was found to be around 700 μm range for natural rubber.

However, further investigations are required to get a higher correspondence between simulations and experiments, and to identify the most critical thermal losses for the performances.

Acknowledgments







This work has been made has a memory of Prof. Jacques JAY, who greatly participate in this project, and sadly passed away at the end of November 2023.

References

[1] M. Sion, J. Jay, G. Coativy, A. Komiya and G. Sebald, Natural rubber based elastocaloric solid-state refrigeration device: design and performances of a single stage system, *J. Phys. Energy* **6** (2024) 02500.3 <https://doi.org/10.1088/2515-7655/ad20f4>

Ferroelectrics under extreme conditions for ultra-high energy conversion

ELyT Global Theme: Energy Scientific topic: Materials and Structures Design

					
Gaspard Taxil ^{1,2,3}	Gaël Sebald ²	Benjamin Ducharne ^{1,2}	Takahito Ono ³	Hiroki Kuwano ^{2,4}	Mickaël Lallart ^{1,*}

¹ Univ. Lyon, INSA-Lyon, LGEF EA682

² ELyTMaX IRL 3757, CNRS, Univ. Lyon, INSA Lyon, Centrale Lyon, Université Claude Bernard Lyon 1, Tohoku University,

³ Graduate School of Engineering, Tohoku University

⁴ New Industry Creation Hatchery Center (NICHe), Tohoku University

Abstract

Energy harvesting has been largely studied due to the possibility to supply low power devices or wireless sensors with residual energy from the environment. A large amount of this residual energy is in the form of mechanical energy that constitutes a ubiquitous source. Ferroelectric materials are very promising for such applications due to their remarkable electromechanical properties. In mechanical energy harvesting, resonant devices operating with vibrating mechanical sources are largely considered. However, there are a lot of random or non-periodic mechanical energy inputs that can be harvested in every day's life (step, tire on road...), leading to the question of how to convert the maximum energy from a single force application. In this work, different ferroelectric materials were experimentally tested and their ultimate energy conversion capacity were determined, ranging 100~400 mJ cm⁻³ per cycle, using Ericsson cycles up to 100MPa and 1.5kV/mm.

The Ericsson cycle starts from a low stress level σ_l and an initial electric field E_i . An electric field is applied until a final value E_f . (1-2 path on Figure. 1(b)). Then, a uniaxial stress is applied to a high value σ_h (2-3 path). Afterwards, the electric field is decreased to its initial value E_i (3-4 path). Finally, the stress is released (4-1 path). An illustration of such Polarization-Electric field cycle is given in Fig. 1(a).

As a proof of concept, a practical application for such high levels of stress and electric field was designed in the form of a smart slab as shown in Fig. 2(a). A given input force of 500~700 N equivalent to the force induced by a human step was amplified by lever effect to reach the targeted stress.

Ericsson cycles were then tested on the slab and an energy output as high as 780 mJ per cycle was achieved (Fig. 2(b)). As a last step, a stand-alone voltage doubler (Bennett doubler) was developed and implemented to provide a realistic application framework while performing thermodynamic cycles at high levels. Energy up to 320 mJ per cycle was obtained (Fig. 2(b)).

Finally, a modelling based on the phenomenological Landau-Devonshire theory was developed. Although primarily used to determine the crystallographic phase of ferroelectric compounds, it was used here to determine the polarization variations induced by both the mechanical stress, the electric field

and the temperature. For the latter case, and working on PMN-PT single crystals, it was proved that the electromechanical converted energy per cycle is weakly dependent on temperature between 20°C and 100°C, followed by a steady decrease when reaching the paraelectric phase.

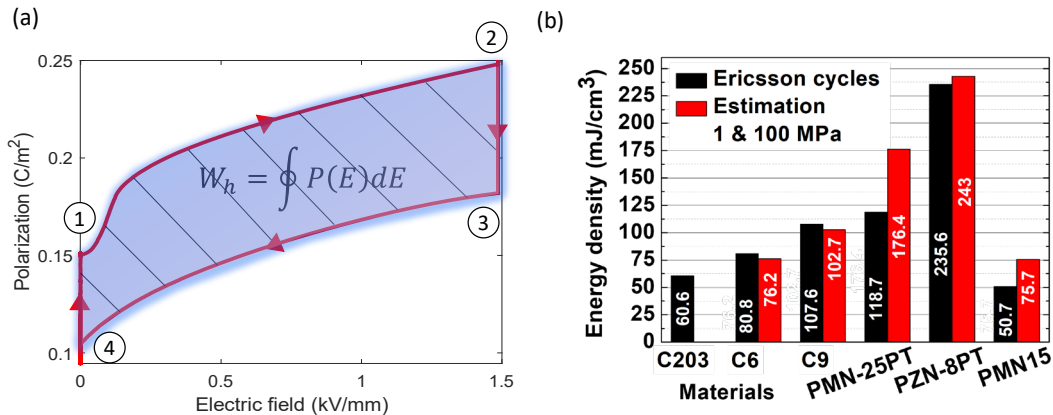


Fig. 1 (a) Example of an Ericsson cycle with the different processes; (b) Comparative diagram of the energy densities of the tested materials

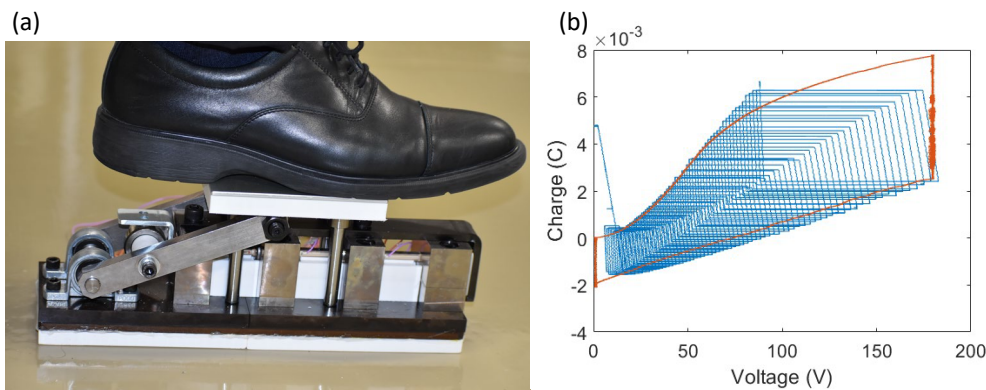


Fig. 2 (a) Illustration of the smart tile; (b) Ericsson cycle (blue) and fully passive Bennet's doubler (blue) under a force of 700 N

On the other hand, it was investigated the effect of the crystallographic direction on the converted energy. PMN-PT single crystal is known to exhibit an ultra-high d_{33} when cut of the polarization axis, thanks to a rotation of the piezoelectric tensor containing an especially large d_{15} . The piezoelectric coefficient d_{33} is then highly direction dependent, with a variation of a factor 20 between the lowest and highest value. Using the phenomenological model, we obtained similar relative variations at low level for the converted energy, being proportional to d_{33} . However, at high level, in-place polarization switching brings much more polarization jumps possibilities. As a consequence, the energy per cycle is much less dependent on the crystallographic direction, suggesting a symmetry breaking when moving from low level to high level case.

Acknowledgement

This work was performed under the framework of the ANR FIESTA project, funded by the French Agence Nationale pour la Recherche, Grant #ANR-20-CE05-0026

References

1. G. Taxil, G. Sebald, T. T. Nguyen, B. Ducharne, H. H. Nguyen, T. Ono, H. Kuwano, M. Lallart, "Stress and electric field induced phase transitions for ultra high energy conversion in ferroelectrics", 2023, *Acta Materialia*, 261, 119367. (doi: 10.1016/j.actamat.2023.119367).
2. G. Sebald, N.T. Tung, G. Taxil, B. Ducharne, J. Chavez, T. Ono, H. Kuwano, E. Lefevre, M. Lallart, "Piezoelectric small scale generator: towards near-Joule output energy generation", 2023, *Smart Materials and Structures*, 32 (8), 085009. (doi: 10.1088/1361-665X/acdf31)
3. N.T. Tung, G. Taxil, H.H. Nguyen, B. Ducharne, M. Lallart, E. Lefevre, H. Kuwano, G. Sebald, "Ultimate electromechanical energy conversion performance and energy storage capacity of ferroelectric materials under high excitation levels", 2022, *Applied Energy*, 326, 119984. (doi: 10.1016/j.apenergy.2022.119984)

Magneto viscoelastic modelling of soft magnetorheological elastomer

ELyT Global Energy – Engineering for Health Materials & Structure Design – Simulation & Modeling



¹LMS, CNRS, Ecole Polytechnique, Palaiseau, France

² SmartTECH Lab. Inc. and ELYTMAX, Tohoku University, Sendai Japan

³ ELYTMAX, CNRS, INSA Lyon, Centrale Lyon, Université Claude Bernard Lyon 1, Tohoku, Sendai, Japan

Abstract

Although the magneto-mechanical coupling of MR elastomers has been experimentally evidenced, the physical mechanisms at the origin of this coupling remained unclear. More specifically, the mechanical behavior shows intriguing features, such as the mechanical losses induced by the magnetic field and nearly frequency independent. To deepen the understanding of the physical insights of the soft MRE, a phenomenological model was developed to catch the coupling behavior of the MRE.

We propose a class of phenomenological models that can model the finite strain viscoelastic response of soft MREs under the application of shear cyclic loads at different mechanical frequencies and strain rates. Extensive experimental campaigns are conducted on the soft MREs under various operating conditions. The models meet the experiments via straightforward calibration thus allowing a comprehensive design framework using optimization codes, finite element full field simulations and device design and realization.

In Fig. 1, we show a comparison between experiments and theoretical predictions for various applied fields b^0 and shear strains amplitudes γ^0 . It is first observed the very important increase of the shear stress with the application of the magnetic field, with an increase by a factor of 3 to 6 depending on the shear strain amplitude, and a much larger increase of the mechanical losses. We observe also clearly that the shape of the curves deviates significantly from that of an elliptical shape, indicating important nonlinear effects at finite strains.

In Fig. 2, we show comparisons between the experiments and model predictions for various shear strain amplitudes. This allows to reveal a Payne-type effect due to finite strains (and not due to frequency as is the usual case) amplified significantly by the presence of the magnetic field. This magnetic Payne effect is revealed by the change of the stress-strain slope at zero shear strain. This slope decreases with increasing the amplitude of the applied shear strain, indicating a form of a long memory (or history) effect in the material. The proposed model is able to reproduce this observation in a fairly good accuracy.

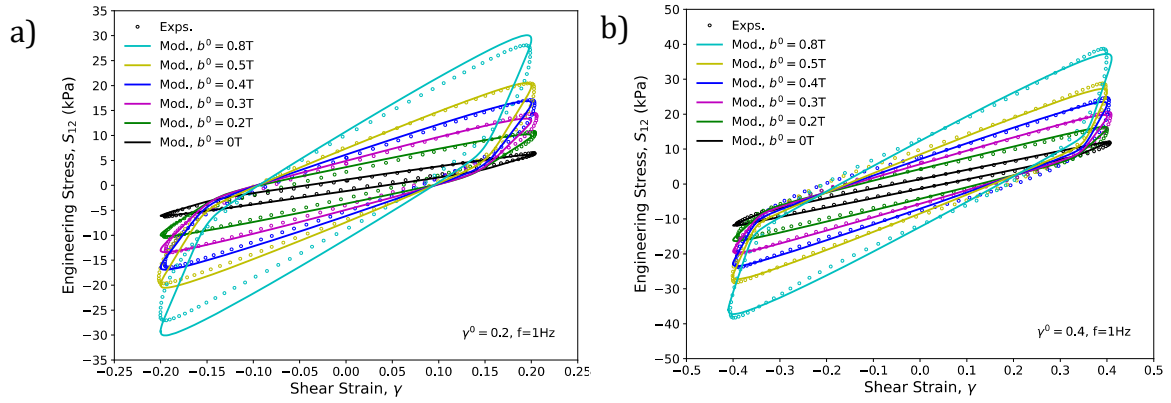


Fig.1 Experiments (markers) versus model predictions (continuous lines) for frequency $f = 1$ Hz and various applied magnetic fields $b^0 = 0, 0.1, 0.2, 0.3, 0.4, 0.5, 0.8$ T for different shear strain amplitudes: a) $\gamma^0 = 0.2$, and b) $\gamma^0 = 0.4$. Note the different range in the y-axes set independently for each plot for better visualization.

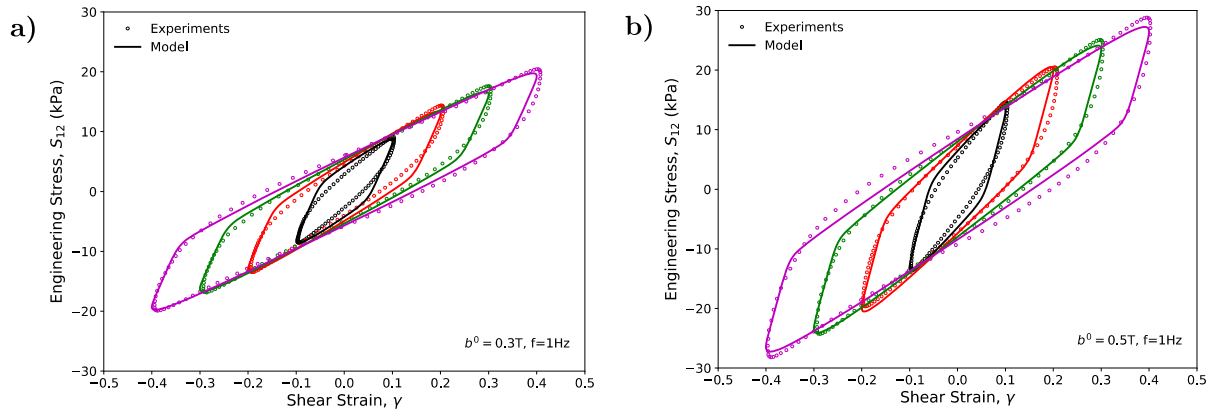


Fig. 2 Experiments (markers) versus model predictions (continuous lines) for frequency $f = 1$ Hz and various shear strain amplitudes $\gamma^0 = 0.1, 0.2, 0.3, 0.4$ for two applied magnetic field amplitudes a) $b^0 = 0.3$ T and b) $b^0 = 0.5$ T.






The magneto-mechanical behavior of a soft matrix MRE revealed complex features. The very important increase of the shear stress and losses with the magnetic field was accompanied by a deviation from the usual viscoelastic behavior of the polymers. In order to catch these features, a mechanical model was developed by writing the equilibrium and non-equilibrium potentials and their dependence on the magnetic field. The model being written intrinsically in tensorial form, it may be used for other simple or complex mechanical loadings.

References

- [1] D. Mukherjee, L. Bodelot, K. Danas, *Int. J. Non-Linear Mechanics*, 120, (2020), 103380.
- [2] S. Lucarini, M.A. Moreno-Mateos, K. Danas, D. Garcia-Gonzalez, *Int. J. Solids Struct.*, 256, (2022), 111981.
- [3] M. Rambašek, D. Mukherjee, K. Danas, *Comp. Meth. App. Mech. Eng.*, 391, (2022), 114500.
- [4] G. Sebald, M. Nakano, M. Lallart, T. Tian, G. Diguët, J-Y. Cavaille, *Science and Technology of Advanced Materials*, 18(1), (2017), 766-778.

Thermal properties versus fibre core microstructure in Vacuum Insulation Panels, towards ageing understanding to ensure ecodesign

**ELyT Global
ENERGY
Materials & Structure design, Simulation & Modeling**

	M. Groux		Prof. C. Le-bourlot
	Prof. P. Dumont		Prof. F. Martoia
	Prof. A. Komiya		Prof. G. Foray

Abstract

Vacuum insulation panels (VIPs) are excellent insulator exhibit thermal conductivity down to $1-2 \text{ mW}\cdot\text{m}^{-1}\cdot\text{K}^{-1}$ that are five times lower than that of the best polyurethane foams ($20-29 \text{ mW}\cdot\text{m}^{-1}\cdot\text{K}^{-1}$) used for domestic appliances. Those are composed of multiple components. VIP market has boomed over the last decade, and still expand ($5.1\%/year$) requiring new core material source (biosourced fibres, recycled mat,..) [1]. VIPs are particularly well-suited for appliance such as refrigerators due to their low thickness. As the first generation of refrigerators equipped with VIPs is now being discarded, it is essential to understand the evolution of these materials to enable the reuse or regeneration of the fibres in the core material.

VIPs thermal conductivity and internal pressure evolve over application time (6 years for cold chain, 60 years for building). Although their performance remains excellent compared to other materials, understanding the mechanisms is crucial to preserve our resource, increase recyclability or promote reversibility. Research has already been conducted on panels, developing experimental and numerical tools to understand dedicated to the silica core panels [2]. Master curve of thermal conductivity versus internal pressure, innovative tools to measure internal pressure on panel, and accelerated core ageing studies under temperature and hygrometry as well as microscopy and X ray tomography on tiny millimetre samples. X ray tomography on full real size VIP panel recently offer the opportunity to view inside a panel. Avenues being explored include analysing the tortuosity and heat transfer paths within the core, a way to image heat flow value measured by heat flux meter. However, these calculations are currently time-intensive, and optimization is required.

Our preliminary study focuses on VIPs with fibrous core materials, aiming to identify the intrinsic mechanisms within the core that contribute to aging. To this end, we analysed several commercial panels aged under in-situ conditions for over 10 years at varying levels of humidity. Using our Double X-ray Tomography Emission (DLTE), we performed X-ray tomography on the entire 400x400x17 mm³ panels at a resolution of 30 microns. We already know that these panels have experienced a change in thermal conductivity from 1.2 to 8.6 mW m⁻¹ K⁻¹. Our scientific aim is to determine the changes the fibrous material and the porous network has undergone to better characterize it.

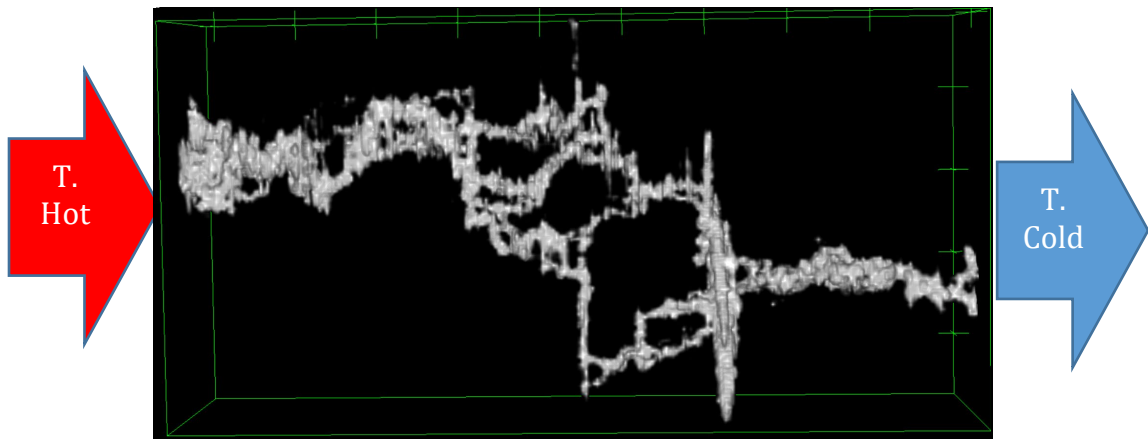


Figure 1 : 3D tomography view of 1% of critical thermal path in a 10y aged VIP with (VIP envelop is set as transparent, 300x100x456 voxels crop, 30 µm resolution. 1.5 computation day for 9mmx3mm surface. Regular vertical fibre hubs change and multiply thermal paths.

However, even if we succeed to study 6 elementary volume (the numerical tools front-growing we currently use is too time-consuming (2.7x2.7 mm² equals 10 days) for panels with surface up to 400x400 mm². We can observe (Figure 1), that a huge pack of fibres attract all paths, thus designing the fibre core matters for ageing. Other approaches, such as the distance map method, are being considered and already yield satisfactory results in terms of computational time.

Moving forward, we will need to validate these new tools to characterize the fibrous core of VIPs. In my doctoral thesis, understanding the relation between aging of fibrous VIPs and the measurement of their thermal conductivities and mechanical properties will enable the exploration of alternative core materials, such as replacing glass fibres with cheaper, potentially recyclable options. After This would allow the use of local, eco-friendly materials. Bio-based materials are a promising alternative, with some studies already demonstrating their potential use in VIPs, like bamboo fibre [3]. However, these studies have not yet addressed the aging of bio-based materials, which are more susceptible to mechanical and textural evolution with humidity than other materials.







[1] « Global Vacuum Insulated Panels Market, 2023-2028 – tanalyze. » Consulté le: 23 janvier 2025. [on ligne]. <https://tanalyze.com/report/global-vacuum-insulated-panels-market-2023-2028/>

[2] S. Brunner et K. Ghazi Wakili, « Hints for an additional aging factor regarding the thermal performance of vacuum insulation panels with pyrogenic silica core », *Vacuum*, vol. 100, p. 4-6, févr. 2014, doi: 10.1016/j.vacuum.2013.07.033.

[3] R. Zhang *et al.*, « Natural fibers as promising core materials of vacuum insulation panels », *Constr. Build. Mater.*, vol. 453, p. 138890, nov. 2024, doi: 10.1016/j.conbuildmat.2024.138890.

**Surface defOrmation acceLerated by hYdrogen Diffusion and
trapping, case of lubrlicated rolling Contact. (SOLYDIC)**

**ELyT Global
Theme (Transportation, Energy)
Scientific topic (Surfaces and interfaces, Materials &
Structure design)**

	<p>Gael ZAVALETA Centrale LYON LTDS</p>		<p>Ana Cecilia PONTES RODRIGUES Centrale Lyon - LTDS</p>
	<p>Nicolas MARY INSA MATEIS</p>		<p>Fabrice VILLE INSA LAMCOS</p>
	<p>Tetsuya UCHIMOTO Tohoku Univ. IFS</p>		<p>Clotilde MINFRAY Centrale LYON-LTDS</p>

Abstract

The industrial sector is developing new products that are less demanding in energy and resources. In the field of ground transportation, this is reflected in the development of electrically powered vehicles, whether the electricity is obtained via a battery or generated by a fuel cell. The use of lubricants is essential for the various systems present in this type of vehicle (electric motor, gears, bearings, etc.). They keep equipment running smoothly, limiting energy losses by minimizing friction and maximizing service life by controlling damage. Depending on the severity of the contact, the lubricant, made up of a base oil and various lubricant additives, can act in different ways: either by establishing an oil film separating the two rubbing surfaces (lubricant film thickness linked to fluid

viscosity and test conditions) or, in the most severe cases, by establishing a tribofilm (film formed on the parts under the effect of friction using additives). But how does hydrogen (H₂), increasingly present in this type of system, affect the tribological behavior of the steel part contacts? What is the influence of the lubricant's nature (base oil and additives)? May the tribofilm act as a barrier to hydrogen diffusion?

This work aims to understand the impact of hydrogen charging of lubricated steel/steel contacts on their tribological behavior, taking into account possible structural changes in the materials, different types of tribological test conditions and the chemistry of the lubricant (base oil and additives).

Preliminary work has shown that steels previously charged with hydrogen (electrochemical charging) increased their wear rate, even in a lubricated environment [1].

The poster will present the experimental strategy proposed to be carried out during Gael Zavaleta's thesis.

The first part of this work will concern the realization of controlled hydrogen charging of steel specimens by electrochemical means with two main objectives:

- to generate specimens with controlled hydrogen content for tribological testing.
- to further understand the interactions between the quantity of hydrogen trapped in steel and the mechanical-physical-chemical modifications induced.

The second part of the project will involve tribological tests using an experimental design that takes into account tribological test conditions (influence of rolling/slip rate, etc.), the quantity of hydrogen pre-charged, the composition of the lubricant, etc. The aim is to understand the impact of hydrogen charging of lubricated steel/steel contacts on their tribological behavior.

All the results put into perspective will enable us to discuss the role of hydrogen in the degradation mechanisms of lubricated steel/steel contacts.

[1] Lisa-Marie Weniger et al., The Effect of Hydrogen Concentration on Surface-Initiated Damage in Rolling Contacts, Luleå University of Technology, Division of Machine Elements (Sweden), 49th Leeds-Lyon symposium of tribology, Ecully France.

**Wednesday,
February 19th**

Afternoon

Principles and applications of ultrasonic transducers

ELyT Global Theme Ultrasonic Scientific topic Non destructive testing



Abstract

Ultrasound, particularly as a diagnostic tool, occupies a major place in the medical and industrial fields, and technological advances and processing capabilities are opening new application fields. In medicine, shear-wave elastography, harmonic imaging, high-frequency imaging [1-4] and 3D imaging are all being explored. In the industrial field, applications are numerous, notably for non-destructive testing and evaluation [5-6]. The nuclear industry is a case in point, where inspection systems often have to be implemented in harsh environments, such as under irradiation or at high temperatures [6] and where the transducer design has to endow these constraints.

With the exception of micromachined capacitive transducers [7], whose operating principle is based on a new technological approach to the piezoelectric transducer, the concept of an ultrasonic transducer has been the same for many years. It is based on the radiation of an ultrasonic wave by a piezoelectric element. One or more intermediate layers can damp the vibrations and adapt the sensitivity and bandwidth to fit the application. This concept is available as a single-element or multi-element transducer.

This presentation examines the main characteristics of an ultrasonic transducer related to electroacoustic response. In many cases, the analytical modeling of a single-element transducer by an equivalent electrical schematic enables transducer design and conception. We therefore examine the effect of the constituent elements of an ultrasonic transducer on its sensitivity, bandwidth and axial resolution.

These elements are used directly in developing and designing transducers for industrial applications. We present the issues at stake and the first results obtained for two types of transducer: an acoustic projector and a high-temperature transducer [8-9]. Finally, we present recent results concerning implementing a method for monitoring hydrogen loading in steel during electrochemical charging [10].

- [1] Y. Deng, N. C. Rouze, M. L. Palmeri and K. R. Nightingale, "Ultrasonic Shear Wave Elasticity Imaging Sequencing and Data Processing Using a Verasonics Research Scanner," in *IEEE Transactions on Ultrasonics, Ferroelectrics, and Frequency Control*, vol. 64, no. 1, pp. 164-176, Jan. 2017, doi: 10.1109/TUFFC.2016.2614944.
- [2] Correia M, Provost J, Chatelin S, Villemain O, Tanter M, Pernot M. Ultrafast Harmonic Coherent Compound (UHCC) Imaging for High Frame Rate Echocardiography and Shear-Wave Elastography. *IEEE Trans Ultrason Ferroelectr Freq Control*. 2016 Mar;63(3):420-31. doi: 10.1109/TUFFC.2016.2530408. Epub 2016 Feb 15. PMID: 26890730; PMCID: PMC4878711.
- [3] S. Catheline, J. -. Thomas, F. Wu and M. A. Fink, "Diffraction field of a low frequency vibrator in soft tissues using transient elastography," in *IEEE Transactions on Ultrasonics, Ferroelectrics, and Frequency Control*, vol. 46, no. 4, pp. 1013-1019, July 1999, doi: 10.1109/58.775668.
- [4] Shung, K. K. High Frequency Ultrasonic Imaging. *J. Med. Ultrasound* 17, 25–30 (2009).
- [5] Baba, A. (馬場淳史), Searfass, C. T. & Tittmann, B. R. High temperature ultrasonic transducer up to 1000 °C using lithium niobate single crystal. *Appl. Phys. Lett.* 97, 232901 (2010).
- [6] D. A. Parks, S. Zhang and B. R. Tittmann, "High-temperature (>500/spl deg C) ultrasonic transducers: an experimental comparison among three candidate piezoelectric materials," in *IEEE Transactions on Ultrasonics, Ferroelectrics, and Frequency Control*, vol. 60, no. 5, pp. 1010-1015, May 2013, doi: 10.1109/TUFFC.2013.2659.
- [7] A. S. Erguri, Yongli Huang, Xuefeng Zhuang, O. Oralkan, G. G. Yarahoglu and B. T. Khuri-Yakub, "Capacitive micromachined ultrasonic transducers: fabrication technology," in *IEEE Transactions on Ultrasonics, Ferroelectrics, and Frequency Control*, vol. 52, no. 12, pp. 2242-2258, Dec. 2005, doi: 10.1109/TUFFC.2005.1563267.
- [8] G. Feuillard, L. P. T. H. Hue, N. Saadaoui, V. T. Nguyen, M. Lethiecq and J. F. Saillant, "Symmetric Reflector Ultrasonic Transducer Modeling and Characterization: Role of the Matching Layer on Electroacoustic Performance," in *IEEE Transactions on Ultrasonics, Ferroelectrics, and Frequency Control*, vol. 68, no. 12, pp. 3608-3615, Dec. 2021, doi: 10.1109/TUFFC.2021.3101124.
- [9] Nguyen, D., Navacchia, F., Tran-Huu-Hue, L., & Feuillard, G. (2022). Ultrasonic characterization, simulation of porous metal in the interest of high frequency applications. Singapore International NDT Conference & Exhibition, November 2022. e-Journal of Nondestructive Testing Vol. 27(12). <https://doi.org/10.58286/27525>
- [10] Louis Leffray . « Etude de la fragilisation par hydrogène des aciers par méthode ultrasonore ». Master thesis. U Le Mans 2024

3D local magnetoresistive probe for magnetic imaging diagnostics

ELyT Global

<p>Aurélie Solignac Service de Physique de l'Etat Condensé, CEA, CNRS, Université Paris-Saclay</p>	<p>W. Benmessaoud¹, L. Drigo³, S. Rouse³, C. Fermon¹, M. Pannetier-Lecoœur¹, M. Macouin³, N. Sergeeva-Chollet²</p> <p><i>¹SPEC, CEA, CNRS, Université Paris-Saclay, CEA Saclay 91191 Gif-sur-Yvette Cedex, France</i></p> <p><i>²CEA LIST, 91191 Gif-sur-Yvette, France</i></p> <p><i>³Géosciences Environnement Toulouse, Université de Toulouse, CNES, CNRS, IRD, UPS, 31400 Toulouse, France</i></p>
--	--

Abstract

Quantitatively, local-scale characterization of the magnetic properties of materials is of great interest for applications such as materials science, nano-metrology, paleomagnetism and nondestructive testing (NDT). In particular, local 3D measurement of magnetic strayfields emitted by a material is a non-destructive means of diagnosing the material or even monitoring its manufacture. A magnetic scanner has been developed, enabling simultaneous and quantitative measurement of the three components of the magnetic strayfields emitted by a material, in static or dynamic field. It is composed by a local 3D probe fabricated with 4 giant magnetoresistance (GMR) sensors placed on the different sides of a pyramidal support, which is scanned over several millimetres or centimetres of sample surface [2] with a lateral resolution of the order of few tens of microns.

Several elements were developed to build the final "Magnetic Scanner with 3D local magnetoresistive probe" measuring instrument: GMRs sensors, 3D probes, measuring electronics as well as the scan and height control setup. On the other, the 3D field reconstruction method relies, in part, on the determination of a sensitivity matrix, characteristic of the measurement and sensors. Simulation and algorithmic calculation techniques have been developed to determine this matrix and propose a reliable and accurate reconstruction of the fields.

Measurements on calibration samples were used to validate the magnetic imaging technique, which was then tested on a number of different materials from a variety of applications, in either static or dynamic fields : magnetic rock thin section for paleomagnetism, steel parts for NDT, nanomagnets for fundamental research and metal parts from additive manufacturing.

After a general introduction on MR sensor, the magnetic scanner will be presented, with special emphasis on sensors optimization, the 3D field reconstruction method and the results obtained on various applications.

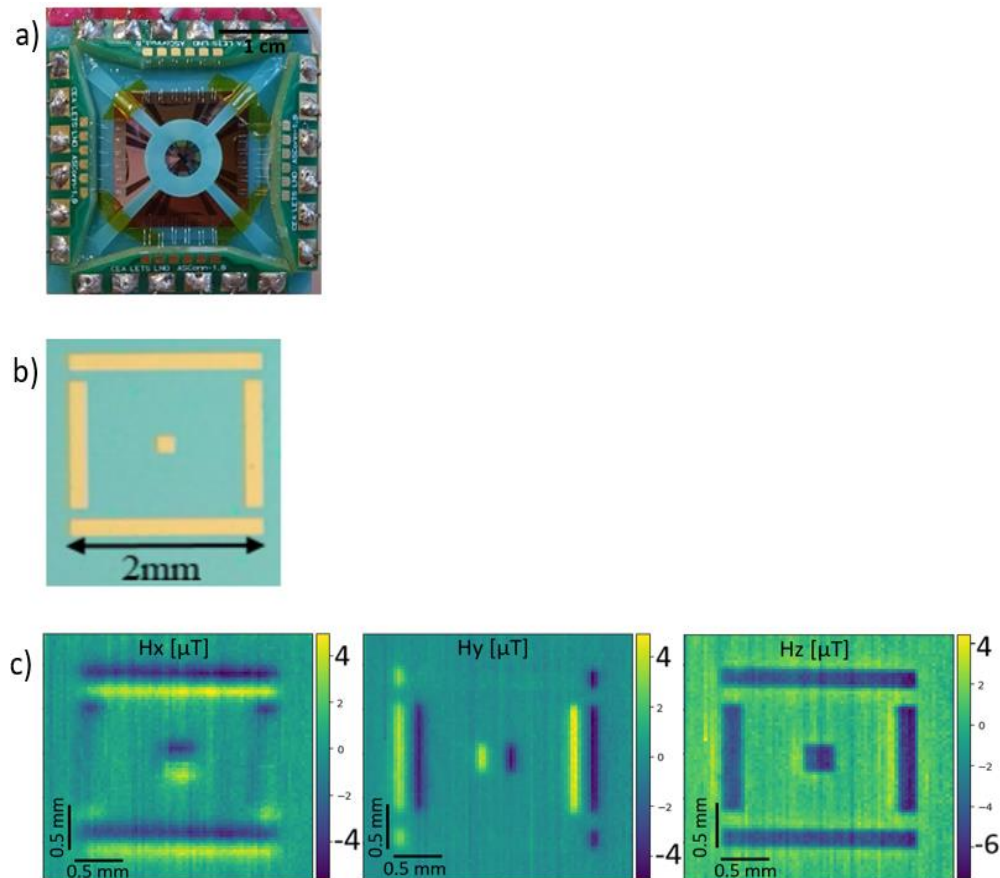


Figure: The 3D local magnetoresistive probe and measurement of a calibration sample obtained with the magnetic scanner. (a) Picture of the 3D local magnetoresistive probe. (b) Picture of the calibration sample : multilayer thin-film of $[(\text{CoFe}_{30}[0.4\text{nm}]/\text{Pt}[1\text{nm}])\times 5]$ with an out of plane perpendicular magnetic anisotropy ($M_{\text{sat}} = 1.7 \times 10^6 \text{ A/m}$). (c) 3D field reconstruction obtained with the magnetic scanner with 3D local magnetoresistive probe.

[1] C. Fermon et al., Noise in GMR and TMR sensors in Giant Magnetoresistance (GMR) Sensors, In: Giant Magnetoresistance (GMR) Sensors. Smart Sensors, Measurement and Instrumentation, Vol 6. Springer, Berlin, Heidelberg, (2013), pp 47–70.

[2] F. Hadadeh, et al., 3D magnetic imaging with GMR sensors, IEEE Sensors Journal, Vol. 19, N°22, (2019).

Controlling friction in rubber materials through advanced strain
measurement and tread design

**ELyT Global
Tribology
Rubber friction**



Abstract

Soft materials, characterized by their ability to deform easily at near room temperature and their elastic modulus below 10 MPa, include synthetic polymers, rubber, gels, and colloids. Among these, rubber stands out for its excellent elasticity and is widely used in industrial applications such as tires, seals, shoe soles, and hoses. The frictional properties of rubber are unique due to its low elastic modulus, viscoelastic properties, and long relaxation times, making the study of friction mechanisms and the development of control technologies essential. This paper introduces the development of strain measurement technology for rubber during sliding friction to elucidate the friction mechanism of rubber materials, as well as the development of high-friction technology for rubber treads in fluid environments utilizing liquid flow.

Improving the braking performance of automobile tires on various road surfaces as well as under wet conditions is a critical challenge. The friction between rubber and rough surfaces, like asphalt roads, involves both adhesive friction and hysteresis friction. Hysteresis friction arises from the stress differences between the compression and recovery processes both on the surface and inside the rubber caused by contact with the mating surface protrusions¹⁾. This phenomenon is particularly pronounced in viscoelastic materials like rubber. Therefore, understanding the strain distribution on and within rubber due to friction is crucial for effective friction control. While numerical simulations have provided insights into strain distribution in rubber during sliding, no experimental method had been developed to measure it. We utilized digital image correlation (DIC) methods to visualize the subsurface strain distribution within silicone rubber sliding against a ball²⁾. By embedding random white dots at different depths in a rubber layer and tracking their positions, three-dimensional strain distribution was measured. This technology is expected to enable the control of hysteresis friction and the design of high-friction tire treads. Research using synchrotron radiation facilities is ongoing to elucidate the

molecular-level friction behavior of rubber. This work aims to establish a foundation for designing high-friction rubber materials at the molecular level.

In Japan, falls in workplace account for a quarter of occupational injuries, with slipping being the primary cause. Factory floors are typically smooth to facilitate cleaning. Consequently, the high-friction effect of hysteresis friction cannot be achieved when the surface is wet. To increase the friction of shoe soles, the depth and direction of tread grooves have been optimized to exclude liquids from the contact interface and enhance adhesion friction. However, the development of rubber treads that provide high friction comparable to dry conditions on wet surfaces has not yet been achieved. We have found that sliding friction between a rectangular rubber tread block and a smooth glass plate in glycerol exhibits a high coefficient of friction exceeding 1.0 under specific conditions. These conditions include a small end-face corner radius of the tread block³⁻⁵⁾ and when the longitudinal direction of the tread block is aligned parallel to the sliding direction⁶⁾. This coefficient of friction is equal to or higher than that of the same rubber tread block under dry friction conditions. Under these high-friction conditions, the rear end of the tread block detaches from the glass surface due to deformation caused by the frictional torque. Consequently, a gap that expands in the direction of slip (expansion gap) is formed between the tread block and the mating surface. Fluid flowing through the expansion gap generates negative fluid pressure. The generation of negative fluid pressure increases the normal force applied between the rubber tread and the mating glass surface. Additionally, the reduction in the thickness of the fluid film causes direct contact between the roughness protrusions at the front end of the rubber tread block and the mating surface. Further experiments with inclined-groove rubber treads demonstrated that grooves designed to generate negative fluid pressure achieved higher friction coefficients in glycerol⁷⁾. Optimizing groove depth and plateau region dimensions enabled even greater friction performance. This technology shows promise not only for slip-resistant shoe soles but also for automobile tire designs to prevent hydroplaning, reducing accidents in wet conditions.

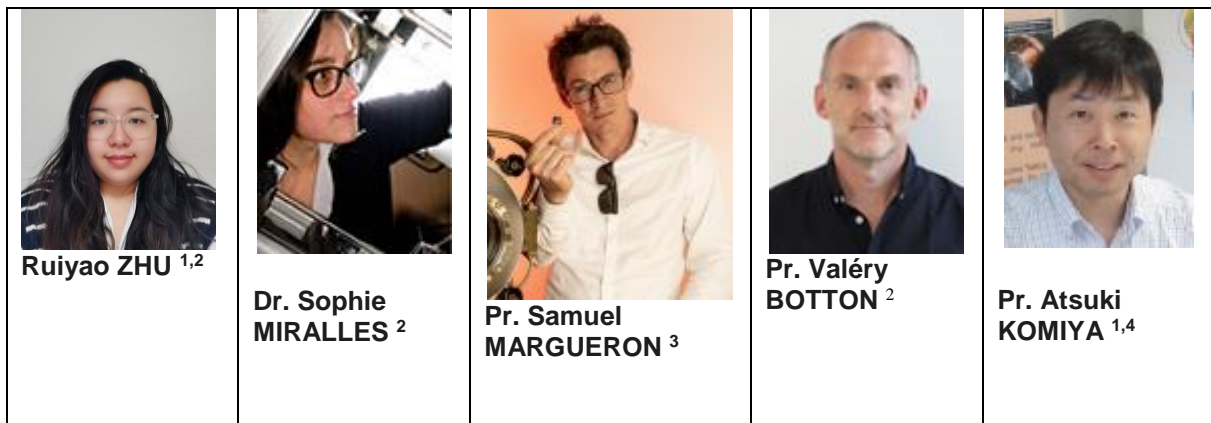
The findings on friction in soft materials extend beyond tires and shoe soles to applications in artificial joints, skin, and other biological tissues. Since human interactions with objects involve soft material friction, elucidating these mechanisms and developing control technologies are of significant importance.

References

- 1) Moore, D. F. *The Friction and Lubrication of Elastomers* (Pergamon Press, 1972).
- 2) Nishi, T., Ueno, K., Nomoto, T., Sugisawa, S., Shin, D., Yamaguchi, K., Kuwayama, I., Yamaguchi, T. Visualization of strain distribution in rubber bulk during friction, *Sci Rep*, 14, 13530 (2024).
- 3) Ishizako, A., Tomosada, M. & Yamaguchi, T. Impact of the end corner face radius of rubber block on friction under dry and lubricated conditions, *Tribol Int* 174, 17705 (2022).
- 4) Ishizako, A., Matsumoto, H. & Yamaguchi, T. Relationship between end-face corner radius of rubber block and friction coefficient and fluid-free gap under lubrication, *Tribol Int* 184, 108473 (2023).
- 5) Ishizako, A., Nishi, T. & Yamaguchi, T. High friction of rubber caused by negative fluid pressure under glycerol lubrication, *Tribol Int* 19, 109213 (2024).
- 6) Ishizako, A., Nishi, T. & Yamaguchi, T. Effect of orientation and hardness of rubber tread block on the friction coefficient under glycerol lubrication and its underlying mechanisms, *Tribol Int* 198, 109904 (2024).
- 7) Ishizako, A., Nishi, T. & Yamaguchi, T. Increasing friction of tread rubber under lubrication by adjusting groove shape to control fluid flow, *Tribology International* accepted.

Towards the Control of Protein Mass Transfer via Ultrasound and Macro-porous Membranes

ELyT Global Engineering for Health Surfaces & Interfaces



¹ Institute of Fluid Science, Tohoku University, Japan

² INSA Lyon, CNRS, Ecole Centrale de Lyon, Université Claude Bernard Lyon 1, Laboratoire de Mécanique des Fluides et d'Acoustique, France

³ Institut FEMTO-ST, CNRS UMR 6174, Université de Franche-Comté, Besançon, France

⁴ ELyTMax IRL 3757, CNRS, Univ. Lyon, INSA Lyon, Centrale Lyon, Université Claude Bernard Lyon 1, Tohoku University, Japan

Abstract

In this study, we are focusing on the precise control of protein mass transfer by using pored membrane and local induced flow. The visualization experiments using a phase-shifting interferometer are performed ([1]), and prior to the study, the effect of pore size and membrane structure was evaluated.

A solution of given protein concentration is injected below the membrane whereas pure water is carefully injected above. The visualization area of the interferometer is located just above the membrane, to measure the evolution of the concentration profile during time (see figure 1).

In this study, several types of the separated membranes were used. As opposed to free diffusion, the membrane pores are hindering the diffusion process. From the concentration profile, the penetrated mass rate in the water side of the membrane has been evaluated. The results show that the size of the pore as well as the size of the molecules are affecting the mass rate

To enhance the mass transfer, the application of an ultrasound induced flow has been performed. In order to generate a flow in the 10 mm cell, an actuator called SAW (Surface Acoustic Wave) device has been used ([2]). The resonant frequencies were either 30.3 MHz or 65.8 MHz. The waves are propagating at the surface of the solid substrate until it reaches the interface between air and water

where the acoustic energy is transmitted to the fluid with a given angle. The attenuation of the acoustic field is then creating momentum, a flow usually called acoustic streaming.

Prior to show the enhancement of mass rate inside the diffusion cell, the acoustic streaming flow has been characterized in a bigger volume using PIV (particle image velocimetry) visualization. As shown in the figure 2, the typical flow is a jet with a fixed angle with respect to the free surface. For moderate values of voltage on the SAW device, several cm/s of maximum velocity is reached around 10 mm from the location of the source. The jet is then radially spreading while the velocity of its axis is decreasing.

In the diffusion cell, the room for the jet flow is limited but the material of the cell (glass quartz) can be used to make acoustic reflections sustaining several jet motions ([3]).

As shown in the results in the figure 3 for a preliminary experiment using salt water, the mass rate through the pored membrane is enhanced by the ultrasound induced flow. The mass rate is clearly increased by the actuation of the ultrasound field.

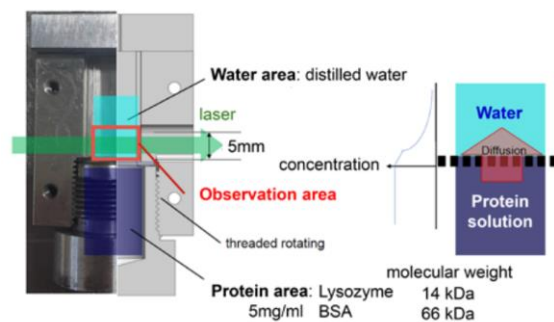


Figure 1 Picture of the observation area in the cell of the phase-shifting interferometer (left). Sketch of the configuration with the concentrated solution, the membrane, and the diffusion area (right).

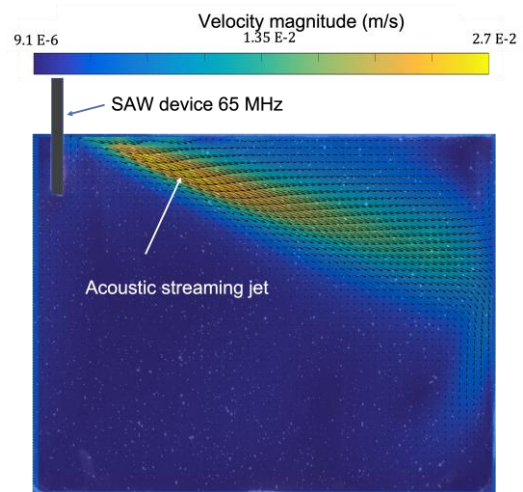


Figure 2 Velocity field visualization (PIV) of the acoustic streaming created by the SAW device at 65.8 MHz in a 50 mm tank of water

References

- [1] Wu et al., *Dynamic imaging and analysis of transient mass transfer process using pixelated-array masked phase-shifting interferometry*, International Journal of Heat and Mass Transfer 174 (2021) 121339
- [2] Dentry et al., *Frequency effects on the scale and behaviour of acoustic streaming*, PHYSICAL REVIEW E 89, 013203 (2014)
- [3] Vincent et al., *Experimental study of helical acoustic streaming flow*, PHYSICAL REVIEW FLUIDS 9, 024101 (2024)

Monitoring Eukaryotic Cell Functions under Various Hypoxic Conditions with Microfluidic Based Oxygenators

ELyT Global Theme: Engineering for Health Scientific topic: Microsystems for cell Engineering

	Prof. Jean- Paul RIEU (ILM, UCBL)		Assoc. Prof. Kenichi FUNAMOTO (IFS, TU)		Associate Professor, Nicolas Aznar (LBTI, CNRS)
---	--	---	--	---	---

Abstract

It is well known that cells sense oxygen (O_2) and change their behaviors accordingly. Cells can move along O_2 gradients toward higher O_2 levels, this aerotactic response used by amoeboid cells moving fast like immune cells or *Dictyostelium* is almost instantaneous. For epithelial or mesenchymal cells like those present in tumors, the hypoxic microenvironment triggers a slow (often genetic) adaptation.

We recently investigated **the aerotactic response of the amoeba *Dictyostelium discoideum* (*Dd*)**. In particular, we developed a double-layer microfluidic device with gas channels and media channels to generate O_2 gradients during cell culture, and we showed that *Dd* amoebae are responding to O_2 gradients in the 0-1.5% O_2 range [1]. To clarify the underlying molecular mechanisms, experimental devices need to be improved in order to perform more experimental conditions in parallel and to control separately the absolute level of O_2 concentration and its spatial gradient. Another cellular model, ***Acanthamoeba castellanii* (*Ac*) has been explored** and compared to *Dd* in order to better understand the mechanisms of aerotaxis.

Multicellular spheroids of cancer cell lines or patient derived organoids constitute a good 3D model of tumors for drug screening and personalized medicine. We are developing **new Organoid-on-Chip platform for 3D organoid culture and 3D imaging under various O_2 Levels**. This project aims to develop a cutting-edge technology allowing to grow colorectal cancer cell spheroids while modulating O_2 tension. The organoid-on-chip device is constituted of a central gel layer where spheroids are injected and two side media channels for constant medium renewing or drug injection [3]. Two gas channels 150 μm above these liquid channels enable the control of a shallow gradient of oxygen between 1% and 21%. The different parts of the device are molded in PDMS and plasma bonded together. A polycarbonate film embedded in the top of the last PDMS part prevents unwanted O_2 permeation [1]. The full O_2 profile inside the device was simulated by Comsol simulations and is currently experimentally verified using O_2 sensing films.

This work was supported by Tohoku University, LyC project 2024 and SHAPE-Med@Lyon.

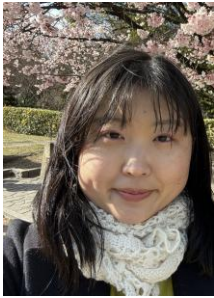




[1] O. Cochet-Escartin, M. Demircigil, S. Hirose, V. Calvez, K. Funamoto, C. Anjard, J.-P. Rieu, *eLife*, 10, (2021), e64731.

[2] S. Hirose, J.-P. Rieu, C. Anjard, O. Cochet-Escartin, K. Funamoto. *Processes*. 10(2), (2022), 318.

[3] K. Funamoto, I. K. Zervantonakis, Y. Liu, C. J. Ochs, and R. D. Kamm, *Lab Chip*. 12, (2012) 4855–4863

Analysis of Guidewire Technique aiming for
Reducing the Load on Vessels at the Internal Carotid Artery Bend

**ELyT Global
Bio-medical Engineering
Evaluation of catheterization procedures**

	<p>Ayami OMIYA Institute of Fluid Science, Graduate School of Biomedical Engineering, Tohoku University</p>		<p>Riko HASEGAWA Institute of Fluid Science, Graduate School of Engineering, Tohoku University</p>
	<p>Hiroyuki KOSUKEGAWA Institute of Fluid Science, Tohoku University Blue Practice Corporation</p>		<p>Prof. Masaaki SHOJIMA Teikyo University Hospital</p>
	<p>Prof. Makoto OHTA Institute of Fluid Science, Tohoku University</p>		

Abstract

Endovascular treatment is attracting attention as a minimally invasive approach in the surgical treatment of stroke. In this treatment, a metal guidewire with a catheter is inserted into the blood vessel, and the catheter is guided to the treatment site. If these devices are pressed too strongly against the vessel wall during insertion, excessive load and friction will damage the vessel wall and lead to complications [1]. To avoid this problem, there is a significant need to

analyze the effects of device manipulation that reduce the load on blood vessels.

In this study, we divided the device manipulation into several elements such as push/pull, insertion speed, and the amount of rotation, aiming to clarify the load applied to the blood vessel in each of these factors.

To replicate the actual endovascular procedure, we developed a catheter robot that can insert a catheter and a guidewire horizontally. The catheter was inserted into a biomodel of a blood vessel, which reproduces the geometry and mechanical properties [2] of the internal carotid artery (ICA) leading to the anterior cerebral artery (ACA). Three strain sensors are equipped on the curved sites of ICA of the biomodel to measure the load applied on the vessel wall during the catheter insertion. In this study, we measured the strain when the guidewire and catheter contacted the vessel wall while the guidewire was rotated clockwise and counterclockwise, respectively.




The results showed that to rotate guidewire could avoid the sudden increase in strain. In addition, we found that an appropriate direction of rotation according to the vessel shape could avoid the sudden increase in strain.

References

1. Yoichi Haga, Hiroshi Yoshida, Tadao Matsunaga, Yasutomo Shimizu, Makoto Ohta, Masaaki Shojima, Taisuke Masuda, Kaihong Yu, Tupin Simon, Chenming Dai, Fumihito Arai, Kanako Harada, "Cerebrovascular Model Equipped with Microsensors", IEEJ Transactions on Sensors and Micromachines, vol.140, No.12, pp.354-362 (2020)
2. Hiroyuki Kosukegawa, Keisuke Mamada, Lei Liu, Kosuke Inoue, Kanju Kuroki, Toshiyuki Hayase, Makoto Ohta, "Measurements of Dynamic Viscoelasticity of Poly (vinyl alcohol) Hydrogel for the Development of Blood Vessel Biomodeling", Journal of Fluid Science and Technology, vol.3, pp.533-543 (2008)

Electromagnetic Tracking of operative Catheter

ELyT Global
**Magnetism application in biomedical
Magnetic tracking system with GMR sensor and
Field-Free-point method.**

		
Prof. Ohta (IFS)	Prof. Ducharne (ElytMax)	Louis Paquet (CREATIS)

Full List of Author:

Louis PAQUET, CREATIS Lyon, France
Makoto OHTA, IFS, Tohoku University, Sendai, Japan
Kevin TSE VE KOON, CREATIS, Lyon, France
Aur lie SOLIGNAC, CEA, Paris-Saclay, France
Noriko TSURUOKA, Graduate School of Engineering, Tohoku University, Sendai, Japan
Yoichi HAGA, Graduate Shool of Biomedical Engineering, Tohoku University, Sendai, Japan
Benjamin Ducharne, ELYTMax, Sendai, Japan

Abstract

X-ray fluoroscopic imaging is the standard method for obtaining catheter position and monitoring the patient's vascular network during catheterization procedures. However, this method exposes both patients and doctors to ionizing radiation. To address this issue, we propose an alternative method for tracking the catheter inside the human body by integrating a magnetic sensor at the catheter tip and generating a known magnetic field

(MF) around the operative zone. The catheter's position can then be determined by measuring this MF.

Due to the mandatory small size of the catheter, we utilized giant-magneto-resistance (GMR) sensors for this tracking system. GMR sensors require only two wires for connection, have a wide bandwidth that allows flexibility in selecting the working frequency and can detect low-intensity MFs down to the nano Tesla range.

Our method is based on the time detection of a moving null MF, known as the Field-Free Point (FFP) for MF generation. This approach requires only a single sensor smaller than $300 \mu\text{m}^2$, making it suitable for any catheter. We constructed an experimental setup to demonstrate the feasibility of this method in one dimension and obtained promising performance results.

**Thursday,
February 20th**

Morning











Ion-doped polymer actuators: experiments and modeling

TEmpuRA Project

ELyT Global

Theme: Materials and structure design

Topic: Energy

	<p>H. Takana 1- Tohoku Univ, Institute of Fluid Science Aoba Ku, 2-1-1 Katahira, Sendai, Miyagi 9808577, Japan</p>		<p>J. Courbon 2- INSA Lyon, Mateis laboratory Bat. Blaise Pascal, 69621 Villeurbanne cedex, France</p>
 <p>3- G. Coativy</p>	 <p>3- L. Seveyrat</p>	 <p>3- V. Perrin</p>	 <p>3- D. Djoumoi</p>
 <p>4- S. Livi</p>	 <p>2- F. Dalmás</p>	 <p>5- G. Sebald</p>	 <p>5,6- J-Y Cavallé</p>

3- INSA Lyon, LGEF lab., EA682, 69621 Villeurbanne cedex, France

4- INSA Lyon, IMP lab., UMR 5223, 69621 Villeurbanne cedex, France

5- ELyTMax IRL3757 CNRS Tohoku University, Sendai, Japan

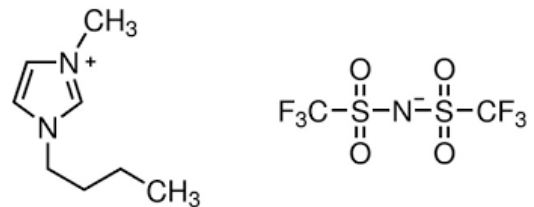
6- Lyon Center, IFS -Tohoku University, 69621 Villeurbanne Cedex, France

Abstract

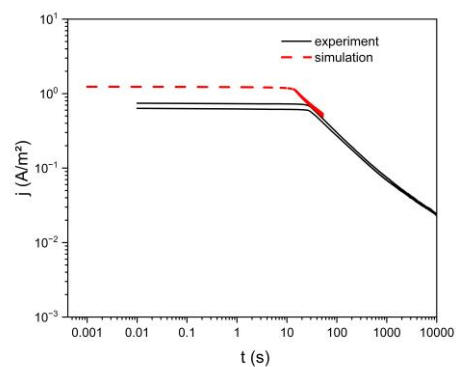
In previous years research on NaCl-containing polyurethane (PU) strips submitted to a high electric field has been conducted [1-3], both on the experimental description of the bending and current density resulting kinetics, as on their modelling. Charge injection models had been first considered [1], then we showed that the main features could be described by an asymmetry of cation vs. anion mobility [2], at least until a threshold of electric field above which charge injection would take place [3] and modify the kinetics. We also were seeking for model materials with controlled microstructure and well-known amounts of charge carriers, and therefore set up a multidisciplinary team involving polymer chemistry, characterization of

bending and ion flow under applied electric field, local material characterization, physical modelling of ion drift and diffusion through the polymer strip thickness and finally mechanical bending under the local Maxwell stress tensor.

Epoxy-amine networks were processed from epoxy prepolymer DGEBA (diglycidyl ether of bisphenol A) with different amount of ionic liquid (IL 1-Butyl-3-methylimidazolium bis(trifluoromethanesulfonyl)imide: in short BMIM TFSI, where BMIM is the cation and TFSI the anion. TFSI is easy to track through the 300 μm -thick strips by means of energy-dispersive X-ray analysis of sulphur and fluor in a scanning electron microscope. Compared to the previous studies on PU, the ion concentration was higher, ranging from 3 to 300 mol/m^3 . It greatly enhanced the conductivity around 1 Hz but did not modify significantly the mechanical properties of epoxy-amine.



As for the simulation of ion segregation kinetics, the applied electric field was lower (often 0.1 MV/m) than on PU. The initial current densities were proportional to the applied electric field, denoting ohmic conductivity as with PU. As expected, the parameters for the drift - diffusion model were reduced to the cation/anion diffusion coefficient ratio, as well as the maximal admissible concentration C_{max} close to the electrodes. The figure shows a fair agreement between simulation and experiment of current density kinetics for



$D_{\text{an}} = 1.5 \cdot 10^{-14} \text{ m}^2/\text{s}$; $D_{\text{cat}} = 2 \cdot 10^{-14} \text{ m}^2/\text{s}$.

However, it seems that some solid-like organization involving at least the anions (unfortunately the cations cannot be traced by EDX) takes place close to the positive electrode. Indeed when removing the applied electric field, the bending amplitude does not decrease to zero while the current density does, denoting some trapping of charge carriers. EDX measurements state that sulphur and fluor segregations persist, while AFM modulus measurements confirm a higher rigidity close to the anode. Further work will be devoted to the understanding of this behavior.

Acknowledgements: the authors would like to thank IFS Lyon-Center (through its Collaborative Research Program) and INSA Lyon (through its Research Quality Bonus (BQR) program) for their support of the TEmPuRA project.








References:

- [1] Bending electrostriction and space-charge distribution in polyurethane films, M. Watanabe, N. Wakimoto, H. Shirai, T. Hirai, *J. Appl. Phys.* 94 2494–7, 2003
- [2] Role of charge carriers in long-term kinetics of polyurethane electroactuation, G Coativy, K Yuse, G Diguët, V Perrin, L Seveyrat, F Dalmas, S Livi, J Courbon, H Takana, JY Cavaillé, *Smart Materials and Structures* 31 (12) 2022, 125019, Doi.org/10.1088/1361-665X/aca12e
- [3] Electric Space Charge Threshold Observation in Polyurethane under High Electric Fields, G. Diguët, J.-Y. Cavaillé, G. Coativy, J. Courbon, *Journal of Applied Physics*, 135 (22), 2024, Doi.org/10.1063/5.0182679
- [4] Effect of ionic liquid on soft epoxy-amine electroactuators, A. Blain, V. Perrin, L. Seveyrat, F. Dalmas, S. Livi, J. Courbon, G. Diguët, H. Takana, J.-Y. Cavaillé, G. Coativy. *Polymer*, 312, 127601, 2024, Doi.org/10.1016/j.polymer.2024.127601

**Application of Electromagnetic Non-Destructive Testing on Steel
Bearing Components:**

SKF-ELyTMaX collaboration

**Joint presentation: Electromagnetic non-destructive testing of steel bearings-
under the Framework of the AB SKF/ELyTMaX collaboration (SAFE project)**

 <p>T. Sulkupuro Knowledge Area Manager NDT/E, AB SKF, Gothenburg</p>	 <p>B. Gupta Senior Process Specialist, Electromagnetic NDT/E, AB SKF, Gothenburg</p>	 <p>J. Hallback Senior Process Specialist, Ultrasound NDT/E, AB SKF, Gothenburg</p>	
 <p>Y.A. Tene Deffo</p>	 <p>G. Sebald</p>	 <p>T. Uchimoto</p>	 <p>B. Ducharne</p>

Abstract

AB SKF is a well renowned manufacturer of steel bearings for aerospace, automotive, energy and general industry. SKF has been a pioneer in terms of quality of the components it delivers to its customers. Hence, the produced components at SKF factories undergo rigorous testing before being deemed 'fit for use'. SKF has a dedicated department on




non-destructive testing and evaluations that ensures the latest developments in the field of NDT/E are deployed in its process control all across its factories globally. SKF has a well established process for the quality control in NDT/E with automated Ultrasound, Eddy Current, Vision methods in place. To stay ahead in quality, SKF is now interested in adopting latest electromagnetic inspection techniques that could provide valuable insights about its bearing components, to make the process of manufacturing even more efficient. By studying the application of Electromagnetic methods, SKF is interested in characterizing its bearings to avoid, if any, grinding burns, or microstructural changes. This investigation will help in further enhancing the quality of components SKF delivers to its customers and improving the manufacturing process as well.

ELyTMaX has extensive expertise in magnetic non-destructive testing (NDT) focused on magnetization mechanisms, which has been developed through years of research and method design. Our work emphasizes creating techniques that isolate magnetization responses specifically sensitive to targeted properties, such as grinding burns and microstructural changes. Equipped with advanced laboratory tools and simulation capabilities, we can effectively link experimental characterizations with magnetic parameters (e.g., magnetic field, magnetization, permeability) to accurately assess properties like grinding burn levels.

Consequently, this potential collaboration will explore alternative techniques, including characterization with a single magnetic probe, a microscopic Barkhausen noise sensor (similar to those in floppy or hard disk readers), a micro coil and lock-in amplifier in a Magnetic Inductive Probe (MIP) configuration, and a Kerr Effect microscope operating in transmitter/receptor mode. The goal is to find the most effective industrially applicable NDE method that could be incorporated in the manufacturing process in the production line.

Incorporating TRIP/TWIP effects in duplex titanium alloys

ELyT Global
Theme: Engineering for Health
Scientific topic: Materials & Structure Design

	<p>Assoc. Prof. Kenta Yamanaka</p> <p>Institute for Materials Research, Tohoku University</p>		<p>Prof. Damien Fabrègue</p> <p>MATEIS, INSA Lyon</p>
	<p>Prof. Akihiko Chiba</p> <p>New Industry Creation Hatchery Center, Tohoku University</p>		

Abstract

The enhancement of strain-hardening ability is crucial for improving the strength-ductility synergy, a longstanding issue for structural metals and alloys [1]. For this purpose, advanced steels have successfully employed two key mechanisms under external loading: transformation-induced plasticity (TRIP) [2], which utilizes strain-induced martensitic transformations, and twinning-induced plasticity (TWIP) [3], which leverages deformation twinning. Recently, these concepts have been adapted to other alloy systems, such as titanium alloys [4] and high-entropy alloys [5], pioneering a novel approach to alloy design. Among them, the newly developed TRIP/TWIP titanium alloys typically consist of single-phase microstructures.

In this study, we successfully incorporated TRIP/TWIP effects into Ti–6Al–4V alloy, the most widely used titanium alloy in industry [6]. A series of heat treatments were conducted below the β -transus temperature to control the composition and mechanical stability of the β -phase within the hexagonal close-packed (hcp) matrix. Through annealing a wrought Ti–6Al–4V alloy at 850 °C (HT-850), followed by water quenching, we obtained a metastable retained β -phase, which contains fewer β -phase stabilizing elements (V and Fe) than the as-received counterpart, with a volume fraction of approximately 25% (Fig. 1).

Figure 2(a) shows the corresponding engineering stress-strain curves for the as-received and HT-850 specimens. Despite a slight decrease in yield stress, the HT-850 specimen exhibits significant work hardening (Fig. 2(b)), consequently enhancing uniform elongation. Transmission electron microscopy revealed that deformation-induced $\beta \rightarrow \alpha''$ martensitic transformation and $(021)_{\alpha''}$ twinning occurred during tensile deformation at room temperature. The results also indicate that the minor retained β -phase could control the macroscopic plastic deformation and contribute to the development of novel alloy designs for enhancing strain hardenability in titanium alloys with fewer alloying elements than recently developed TRIP/TWIP β -Ti alloys.

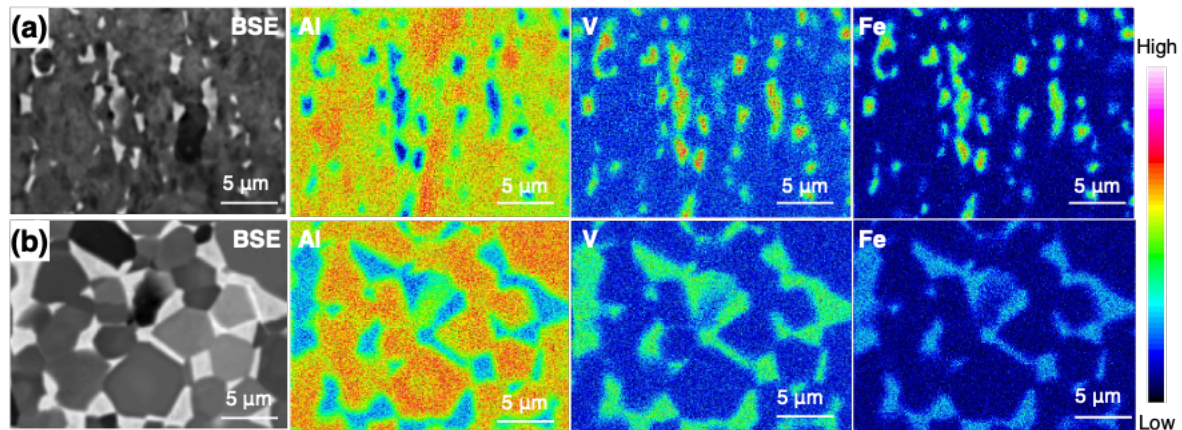


Figure 1. SEM-BSE images and corresponding elemental maps of the (a) as-received and (b) HT-850 specimens.

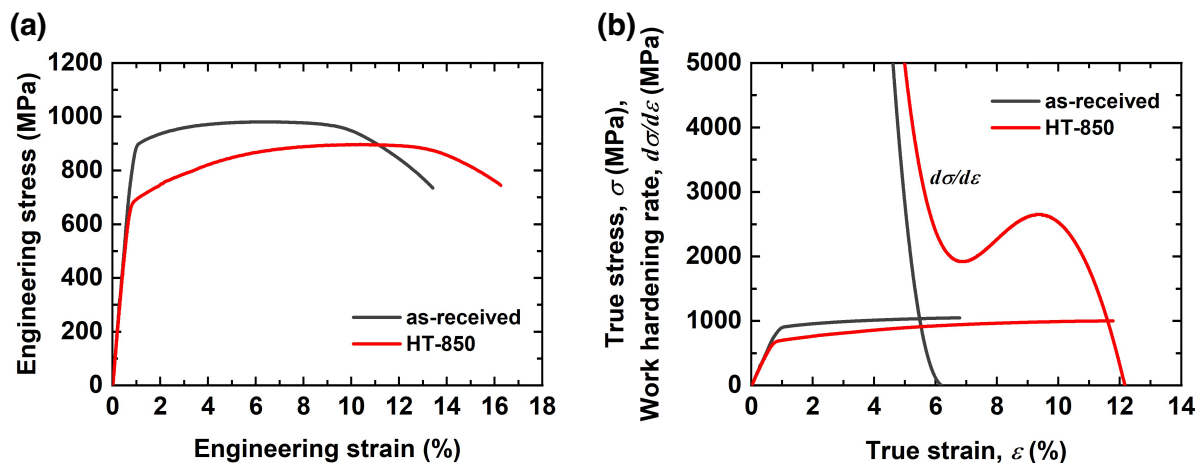







Figure 2. (a) Engineering stress-engineering strain curves and (b) true stress (σ) and work-hardening rate ($d\sigma/d\varepsilon$) as a function of true strain (ε) of the as-received and HT-850.

References

- [1] N. Tsuji et al., *Scr. Mater.* 181 (2020) 35–42.
- [2] M. Soleimani, A. Kalhor, H. Mirzadeh, *Mater. Sci. Eng. A* 795 (2020) 140023.
- [3] B.C. De Cooman, Y. Estrin, S.K. Kim, *Acta Mater.* 142 (2018) 283–362.
- [4] M. Marteleur et al., *Scr. Mater.* 66 (2012) 749–752.
- [5] Z. Li, K.G. Pradeep, Y. Deng, D. Raabe, C.C. Tasan, *Nature* 534 (2016) 227–230.
- [6] K.S.N. Sessa et al., *Mater. Res. Lett.* 10 (2022) 754–761.

**Electric Field Dependence of Parameters Related to the C Diffusivity
in Steel and Improvement of Previous Analytical Model**

**ELyT Global
Theme : Energy
Scientific topic : Simulation and modelling**

	<p>Mr. R. Onozuka (Institute of Fluid Science, Tohoku University, Japan) , (Graduate School of Engineers, Tohoku University, Japan)</p>		<p>Dr. C. Adessi (Institut Lumière Matière, University Claude Bernard Lyon 1, France)</p>
	<p>Prof. J. Kioseoglou (COSSPHY, Theoretical and Computational Solid State Physics, Aristotle University of Thessaloniki, Greece)</p>		<p>Prof. P. Chantrenne (MATEIS, INSA-Lyon, France)</p>
	<p>Prof. T. Tokumasu (Institute of Fluid Science, Tohoku University, Japan)</p>		

Abstract

Recently, thermal treatment processes that utilize electricity generated from renewable energy (e.g., Induction Heating (IH)) have been attracting a lot of attention in the industry because of their ability to reduce CO₂ emissions during the processes. Unlike usual thermal treatment processes, which rely only on thermal diffusion (e.g., burner or furnace), the above-mentioned processes involve both thermal diffusion and electromigration. Therefore, the phenomena become more complex than usual thermal treatment processes. As a result, simulation of these

processes becomes more challenging, due to a lack of knowledge for the processes. Specifically in the case of Fe-C alloys, the diffusivity of carbon is relatively high so analyzing the diffusion coefficient of carbon is important.

In a previous study^[1], it was revealed that the drift velocity of carbon atoms in the direction of the electric field does not follow the Nernst-Einstein relation as the electric field intensity increases. Assuming that diffusivity depends on the electric field, the possibility that parameters related to diffusivity have electric field dependence has been investigated until now. Previous radial distribution function results^[1] indicate that the energy barrier for the jump was unaffected by the electric field. Based on the Arrhenius equation, the remaining parameter influencing the diffusivity is the pre-exponential factor, which is closely related to the attempt frequency.

In a prior study^[2], an analytical model was developed to calculate the drift velocity using the attempt frequency, but the model underestimated the drift velocity compared to that obtained from the slope of the displacement in the direction of the electric field. One reason for this underestimation may be that the model was based on a one-dimensional(1D) Maxwell distribution (Fig. 1(a)). In reality, as shown in Fig. 1(b), carbon moves three-dimensionally in the Fe crystal. Therefore, a three-dimensional(3D) Maxwell distribution was needed to more accurately represent this behavior. This may be one of the reasons why the drift velocity was underestimated. In this study, the previous model was improved to account for 3D movement. The results are shown in Fig. 2. In Fig. 2 the blue markers represent the drift velocity obtained from the slope of carbon displacement, red solid line represents the Nernst-Einstein relation, green solid line represents the 1D Maxwell distribution-based model and violet solid line represents the 3D Maxwell distribution-based model.

From these results, it can be seen that 3D Maxwell distribution-model shows a clear improvement over the 1D Maxwell distribution-model. However, discrepancies still remain. One possible reason for this remaining discrepancy is that there is further room for improvement in the analytical model itself. Another possible reason is that the attempt frequency may have electric field dependence. The drift velocity may have been underestimated because the attempt frequency used was obtained under conditions without an electric field. In future work, the attempt frequency will be directly analyzed under an electric field using Fourier transform.

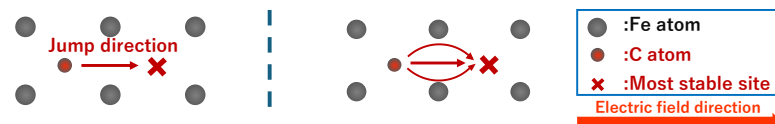


Fig. 1(a) 1D diffusion

Fig. 1(b) 3D diffusion (Realistic Diffusion)

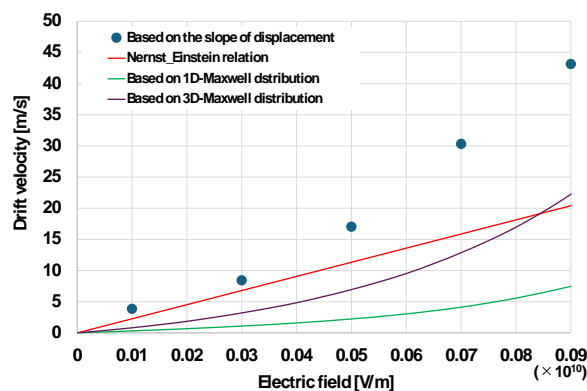


Fig. 2 Drift velocity

[1] R. Onozuka, P. Chantrenne, T. Tokumasu, *Proc. Twentieth International Conference on Flow Dynamics*, (2024).

[2] R. Onozuka, P. Chantrenne, T. Tokumasu, *Extended Abstracts of The Third Pacific Rim Thermal Engineering Conference*, (2024).

**Thursday,
February 20th**

Afternoon

Interfacial Thermal Resistance at Solid-Liquid Interfaces with Complex Morphologies: Evaluation and Interpretation via Molecular Dynamics



^a *Institute of Fluid Science, Tohoku University, 980-8577, Sendai, Japan*

^b *Graduate School of Engineering, Osaka University, 565-0871, Osaka, Japan*

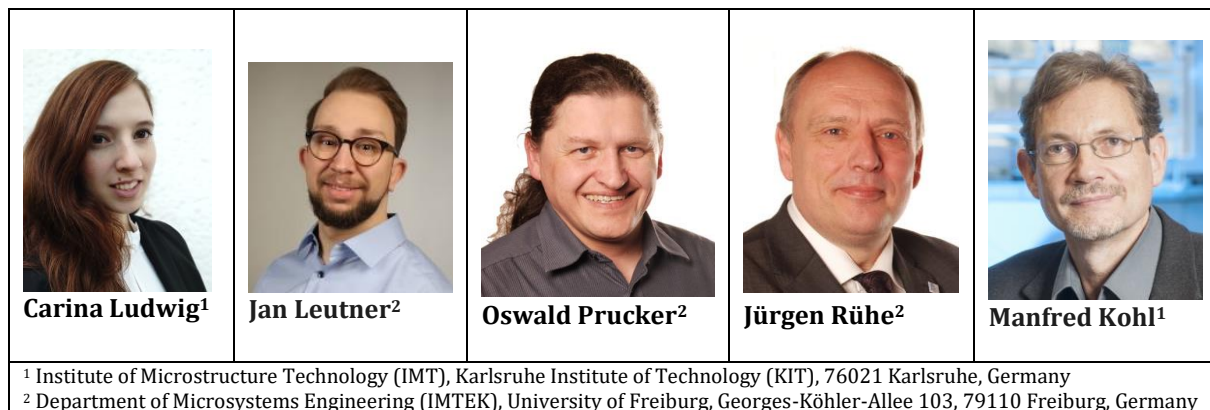
Abstract

Molecular dynamics (MD) simulations are frequently used to estimate interfacial thermal conductance (ITC). By imposing a heat flux and creating non-equilibrium systems (NEMD), the temperature jump at the interface is measured, and the interfacial thermal resistance is calculated using Fourier's law. This method is widely used; however, uncertainties arise with complex surfaces, such as interfacial position, and thus the temperature jump can no-longer be determined unambiguously. Another method, independent of the exact interfacial position, is used with systems under equilibrium (EMD), where the self-correlation of interfacial heat flux is used to obtain ITC via the Green-Kubo (GK) relation. Both approaches were used on systems with flat and grooved solid-liquid interfaces under various solid-liquid interaction strengths, covering a range from very poor to super wettability.

It was discovered that ITC of grooved systems obtained via the GK relation in EMD only reflected the increase in interfacial contact area, while ITC per unit area remained unchanged, while this was not the case for the NEMD approach. This resulted in the EMD approach underestimating ITC values when compared to NEMD. Therefore, we have demonstrated that the EMD approach only reflects the immediate interfacial effects, failing to reflect the overall ITC, while NEMD is more encompassing. In addition, the EMD approach underestimated ITC even in flat interface systems under strong solid-liquid interactions, which can be explained by creation of distinct adsorption structures by liquid atoms, which have a significant effect on interfacial heat transfer, while not necessarily influencing the immediate solid-liquid interface.

Natural Rubber Foil-Based Elastocaloric Cooling using Bistable Actuation

ELyT Global Theme: Elastocaloric Cooling (eC) Scientific topic - Material and device design



Abstract

We introduce a miniature-scale elastocaloric cooling (eC) device utilizing a bistable actuation mechanism for load cycling of a natural rubber (NR) foil refrigerant with lateral dimensions of 9×26.5 mm². The large surface-to-volume ratio of rubber foils facilitates heat transfer to the planar heat sink and heat source through solid-to-solid contact. Employing a single-stage design, the device incorporates a rotating lever arm providing for stable positions with good thermal contact, which allows for significant power saving. The effect of operating parameters and NR foil thickness on performance metrics, including cooling power, temperature span and coefficient of performance (COP) are analyzed.

1. Introduction

Cooling applications account for approximately 17% of global electricity consumption, while most systems relying on vapor-compression devices with high global warming potential (GWP). Elastocaloric (EC) cooling, utilizing superelastic shape memory alloys (SMAs), has emerged as a promising alternative due to their efficient phase transformation. Previous work on SMA films have demonstrated significant potential for miniature-scale cooling applications, such as electronics and lab-on-chips, achieving a cooling power of 19 Wg^{-1} and a temperature span of 27.3 K. [1,2]. However, challenges such as high stress requirements, material availability, and costs limit their broader use. Natural rubber (NR) elastomers present a cost-effective and environmentally friendly alternative, with advantages like low loading forces, excellent fatigue resistance, and a large adiabatic temperature change of ~ 20 K. A few studies have been reported focusing on NR foil refrigerants with a large surface to volume ratio to enable the separation of heat and cold through solid-to-solid heat transfer [3,4]. Here, we introduce a novel bistable actuation mechanism for load cycling and explore the resulting EC cooling performance.

2. Device operation mechanism

Fig. 1a) illustrates the bistable actuation mechanism of the EC device based on an inverse Brayton cycle, requiring only one actuator to load the NR foil refrigerant [4]. A rotating lever arm is introduced to

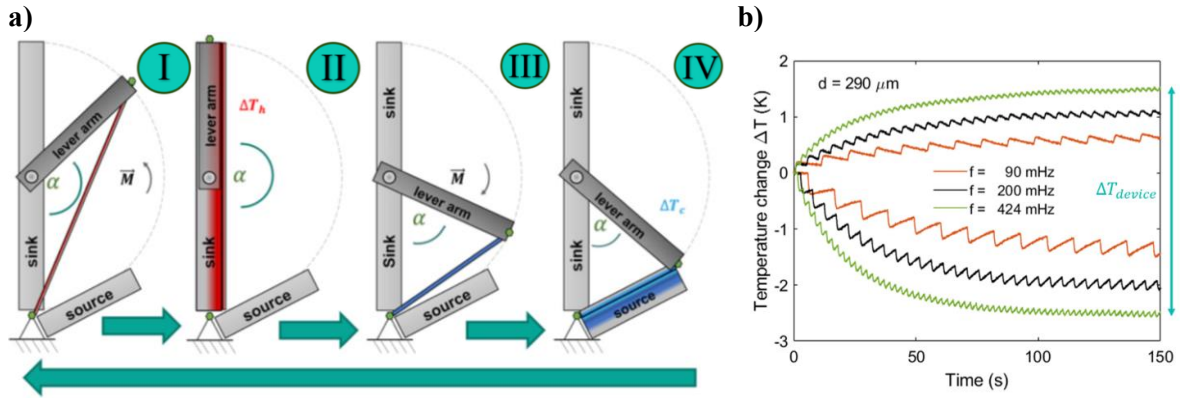


Figure 1: a) Schematic illustrating the EC cycle in four steps employing bistable actuation with a rotating lever arm. b) The temperature evolution of heat sink and source at different frequencies as indicated. Reproduced from [5], licensed under CC BY.

enable bistable actuation. The EC cycle consists of four steps: mechanical loading of the NR foil under quasi-adiabatic conditions (I), heat transfer to the heat sink (II), subsequent quasi-adiabatic unloading (III), and cooling of the heat source (IV). The loading and unloading times are adjusted, with heat transfer occurring during the stable end positions at 300% and 700% strain. Typical temperature evolutions of the device are given in Fig. 1b) at different frequencies for a foil thickness of 290 μm . After the initial temperature change saturation occurs after about 75 s. The device temperature span ΔT_{device} reaches a maximum of about 4.2 K.






3. Results

The impact of different maximum strain levels, pre-strain, and strain rates on the temperature output are analyzed under uniaxial tensile loading. Strain ranges of 300%-700% are identified as optimal due to strain-induced crystallization (SIC) resulting in a temperature change of the material of +6/-8 K at a strain rate of 9.3 s^{-1} . The high strain rate is needed to reach adiabatic conditions. NR foil thicknesses are 290 and 650 μm in their undeformed state. The thickness reduces to 270/150 μm at the pre-strain of 300% and reaches 180/80 μm at the maximum strain of 700%. Due to the bistable mechanism, only the tangential force component needs to be provided by the actuator for load cycling. Thus, the maximum required force for actuation reduces by a factor of 2.8 (650 μm) and 2.5 (290 μm). No power input is needed during the time periods of contact to the heat sink and source, in which the actuator rests in the stable end positions. For the 290 μm thick NR foil, 64% of the total cycling time occurs without power input at the optimal frequency of 424 mHz. The performance of cooling power and $\text{COP}_{\text{device}}$, shows a strong dependence on the foil thickness. As the thickness decreases from 650 to 290 μm , the optimal operating frequency rises from 350 to 424 mHz. Consequently, the cooling power increases from 158 to 214 mW corresponding to maximum specific cooling power values of 1.1 and 3.4 W g^{-1} , respectively. The $\text{COP}_{\text{device}}$ reaches a maximum of 5.7 for the 290 μm thick NR foils. The experimental temperature changes are compared with lumped-element (LEM) simulations indicating that tailoring of heat transfer has a large potential for further improvement of cooling power.

- [1] F. Brüderlin, L. Bumke, C. Chluba, H. Ossmer, E. Quandt, und M. Kohl, „Elastocaloric Cooling on the Miniature Scale: A Review on Materials and Device Engineering“, Energy Technol., Bd. 6, Nr. 8, S. 1588–1604, 2018, doi: 10.1002/ente.201800137.
- [2] F. Brüderlin, „Advanced Elastocaloric Cooling Devices Based on Shape Memory Alloy Films“, 2022. doi: 10.5445/KSP/1000125495.
- [3] C. Ludwig, J. Leutner, O. Prucker, J. Rühle, and M. Kohl, “Miniature-scale elastocaloric cooling by rubber-based foils,” JPhys Energy, vol. 6, no. 1, p. 015009, Nov. 2023, doi: 10.1088/2515-7655/ad0cff.
- [4] M. Sion, J. Jay, G. Coativy, A. Komiya, and G. Sebald, “Natural rubber based elastocaloric solid-state refrigeration device: design and performances of a single stage system,” J. Phys. Energy, vol. 6, no. 2, p. 025003, Feb. 2024, doi: 10.1088/2515-7655/ad20f4.
- [5] C. Ludwig and M. Kohl, “Bistability-enhanced elastocaloric cooling device based on a natural rubber foil,” Journal of Applied Physics, vol. 136, no. 16, p. 165001, Oct. 2024, doi: 10.1063/5.0231213.

Heat transfer control for solid-state refrigeration using natural rubber

ELyT Global Theme: Energy Scientific topic: Materials and Structures Design

				
Atsuki KOMIYA ^{a,b}	Gaël SEBALD ^a	Marianne SION ^{a,b,c}	Shihe XIN ^c	Gildas COATIVY ^d

^a *ELyTMaX IRL 3757, CNRS, Univ. Lyon, INSA Lyon, Centrale Lyon, Université Claude Bernard Lyon 1, Tohoku University, Sendai, Japan*

^b *Institute of Fluid Science, Tohoku University, Sendai, Japan*

^c *CETHIL UMR5008, F-69621, INSA-Lyon, CNRS, Université Claude Bernard Lyon 1, Villeurbanne, France*

^d *INSA Lyon, LGEF, UR682, Villeurbanne, France*

Abstract

Space cooling and refrigeration are based mostly on vapor-compression of a refrigerant gas. Since the early development of this technology in the late 19th century, 3 successive generations of refrigerants were utilized to solve performance, toxicity, flammability, or environmental issues. The 4th generation still did not emerge since 1997 (Kyoto protocol) despite the decision to phase out the currently used HFC. Alternatively, recent research suggests that solid refrigerants deserve more attention although. In this context, we investigated natural rubber as a solid refrigerant, both through material characterization and the development of experimental proofs of concept. Compared to other solid refrigerants, natural rubber exhibits numerous advantages, such as abundance, low cost, and low CO₂ footprint (one or two orders of magnitude compared to metals). Large scale development is then foreseen to be plausible. In the presentation, several recent actions of the REFRESH project will be introduced. Several types of devices were developed. The first one is a so-called single-stage proof of concept, where a rubber sheet is subjected to a four-step process. Another poster presentation details the device and will not be detailed here.

Instead of using solid-solid heat exchange and physically moving the solid refrigerant, another way is to use a heat transfer fluid. A structure composed of 55 natural tubes was assembled allowing to parallelize the cooling power of each single tube [1]. The tubes are connected to reservoirs, collecting the heat transfer fluid after passing inside the tubes. The device is then subjected to a four-step process: (1) stretching of the natural rubber tubes inducing their temperature increase, (2) displacement of the heat transfer fluid through the rubber tubes toward the hot heat exchanger, (3) un-stretching of the tubes inducing a temperature decrease, and (4) displacement of the heat transfer fluid through the rubber tubes and towards the cold heat exchanger.

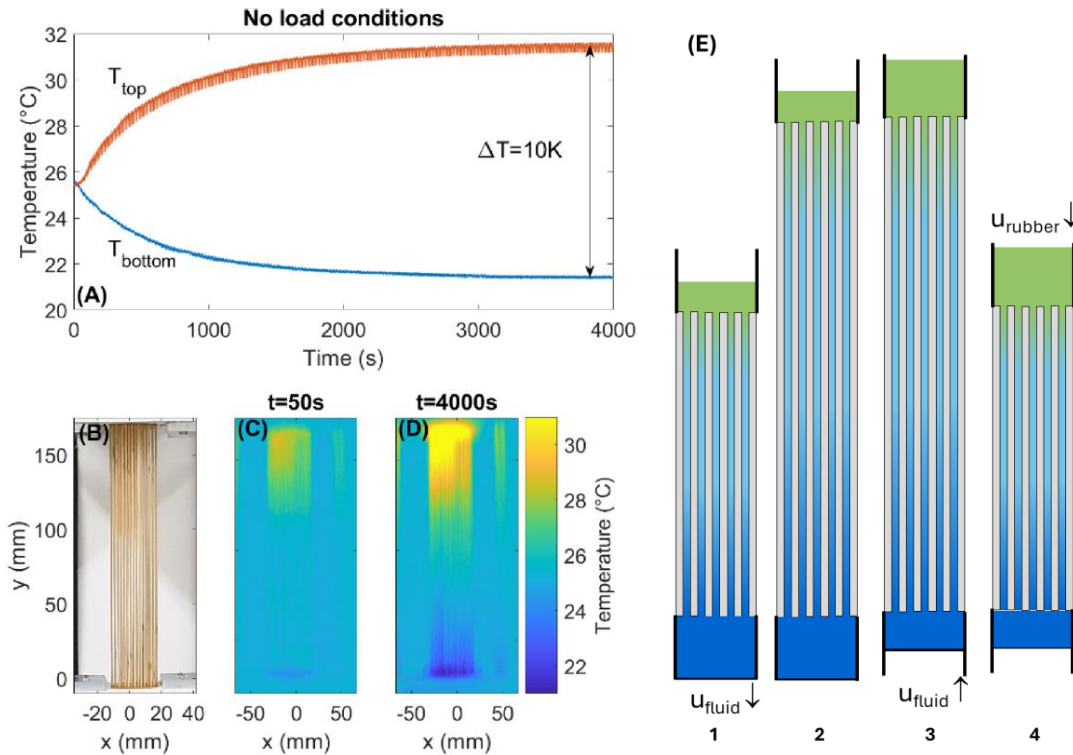


Fig. 1 Elastocaloric rubber cooler performances. (A) Measurement of the temperature span under unloaded conditions with insulated reservoirs. (B) Photograph of the regenerator with (C) its corresponding surface temperature after 50 s and (D) after 4000 s. (E) Four-step cycles for refrigeration. After [1].

The geometry was adjusted according to the thickness of the thermal boundary layer in harmonic regime [2]. The maximum achieved temperature span was 10 K, while the maximum cooling power was found to be 1.8 W. The heat transfers were then more deeply investigated by testing various operating conditions on a single tube experiment, like the impact of the waveforms of the displacements, or the effect of the thermal losses by convection.

Finally, the refrigeration function was reversed, to be able to convert heat into mechanical energy. The objective was to first quantify the energy that can be converted by natural rubber, and then to determine the potential of valorization of low-grade heat. By cyclically injecting hot and cold fluid in the tubes, variations of the stress were induced. It was found that the stress variations were around $5\text{-}10 \text{ kPa}\cdot\text{K}^{-1}$ when pre-stretched over a wide temperature range (15°C to 75°C), a value that was found to be consistent with the elastocaloric activity (i.e variations of entropy driven by the elongation). The same four-step process was applied to the device, but by inverting the hot and cold heat exchangers. Active energy conversion cycles were then obtained and led to the first estimation of the energy density that can be converted by natural rubber thanks to its thermomechanical properties. It was found the natural rubber can convert up to $150 \text{ mJ}/\text{cm}^3$, which was found comparable to the energy conversion in bulk ferroelectrics (both piezoelectric and pyroelectric energy conversion).



Acknowledgements

This work was partially supported by ANR (project ECPOR ANR-17-CE05-0016), and by the JSPS (Grant-in-Aid for Scientific Research grant no. 19K04230).

Reference

- [1] Sebald G, Lombardi G, Coativy G, Jay J, Lebrun L, Komiya A, Appl. Therm. Eng., 223, (2023), 120016.
- [2] Sebald G, Komiya A, Jay J, Coativy G, Lebrun L, J. Appl. Phys., 127, (2020), 094903.

Organic LEDs Based on Bis(8-hydroxyquinoline) Zinc Derivatives**ELyT Global
Theme Energy
Scientific topic Materials and structure design**

	<p>Dr Alexandra Apostoluk</p> <p>Université de Lyon, INL-INSA Lyon, CNRS, UMR 5270, 69621 Villeurbanne, France</p>		<p>Dr Malgorzata Sypniewska</p> <p>Bydgoszcz University of Science and Technology, Faculty of Chemical Technology and Engineering, Bydgoszcz, Poland</p>
	<p>Prof. Beata Derkowska- Zielinska</p> <p>Nicolaus Copernicus University, Institute of Physics, Torun, Poland</p>		<p>Prof. Bruno Masenelli</p> <p>Université de Lyon, INL-INSA Lyon, CNRS, UMR 5270, 69621 Villeurbanne, France</p>

Abstract

(8-hydroxyquinoline) aluminum (Alq₃) derivatives play an important role in the applications in green organic light-emitting diodes (OLEDs). The goal of this work is to investigate the optical and morphological properties of polymer matrix thin layers containing bis(8-hydroxyquinoline) zinc with a styryl group ZnStq_R with various substituents (R = H, Cl, OCH₃, see Fig.1) using UV-Vis and IR spectroscopies, SEM and photoluminescence (PL). Layers were deposited on silicon substrate using the spin-coating method.

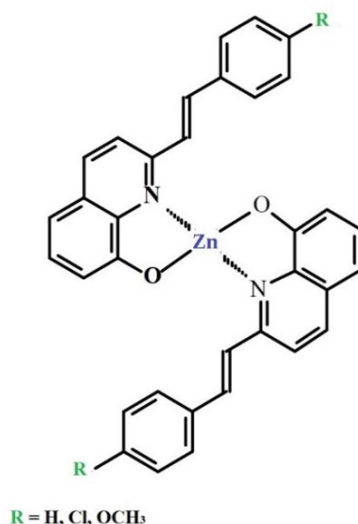


Fig. 1. Chemical structure of ZnStq_R complexes, where R = H, Cl, OCH₃.

We discuss the effects of the each substituent (R = H, Cl, OCH₃) on the film morphology and on the enhancement of the luminescent emission efficiency. Various spectral contributions to the luminescent emission were also examined (Fig.2), in order to achieve a control of the color emission and possibly to increase its efficiency. The produced OLEDs showed strong electroluminescence with yellow emissions at 590, 587 and 578 nm for the ZnStq_H:PVK, ZnStq_{Cl}:PVK and ZnStq_{OCH₃}:PVK, respectively. Obtained maximal brightness for each fabricated OLED was as follows : 2595 cd/m² for ZnStq_H, 1793 cd/m² for ZnStq_{Cl} and 2244 cd/m² for ZnStq_{OCH₃} [1].

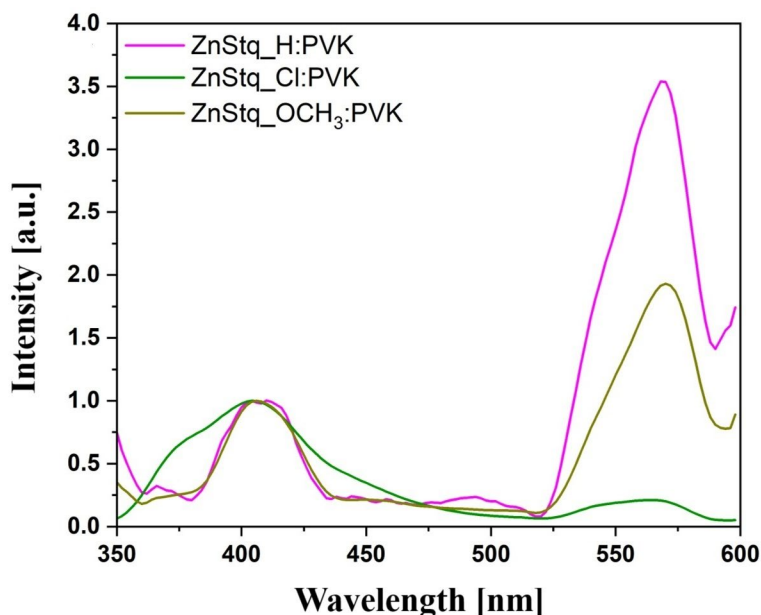


Fig. 2. Photoluminescence spectra of ZnStq_R dispersed in PVK matrices.

References :

[1] Molecules 2023, 28(21), 7435; <https://doi.org/10.3390/molecules28217435>

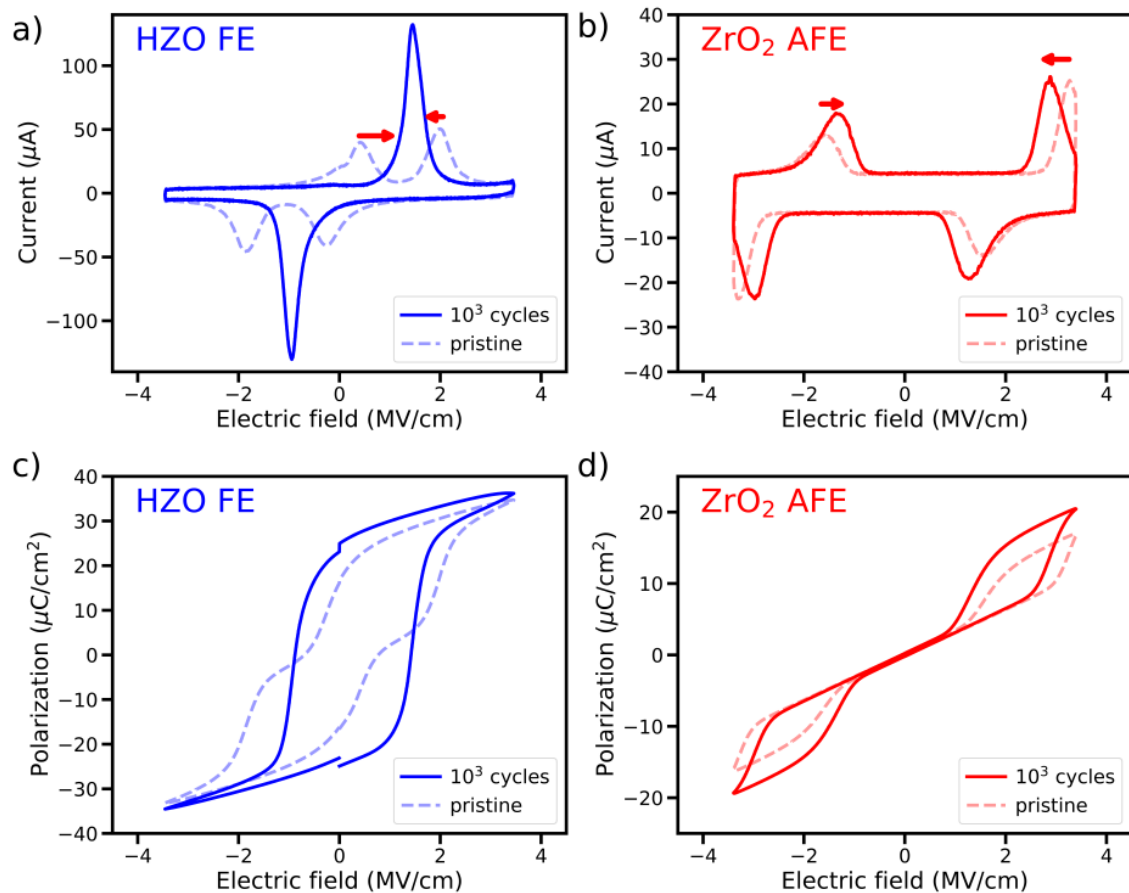
Nanoscaled ferroelectric binary oxide thin film supercapacitors for flexible and ultrafast pulsed power electronics

**ELyT Global
Energy
Materials design**



Abstract

Immediate remedies are essential to address the challenges posed by the exponential increase of energy consumption. Specifically, pivotal technologies related to the fourth industrial revolution—such as the Internet of Things and Big Data—are witnessing an exponential surge in energy consumption linked to the storage, processing, and transmission of digital information [1]. Harnessing the potential of ferroelectric (FE) and antiferroelectric (AFE) materials compatible with complementary metal–oxide–semiconductor (CMOS) technology is a compelling strategy for the creation of energy-efficient electronic devices more specifically for energy conversion applications [2]. Over the last fifteen years, ferroelectric and antiferroelectric ultrathin films based on fluorite-structured materials have drawn significant attention for a wide variety of applications requiring high integration density. Antiferroelectric ZrO_2 , in particular, holds significant promise for nanosupercapacitors, owing to its potential for high energy storage density (ESD) and high efficiency (η). This work assesses the potential of high-performance $\text{Hf}_{1-x}\text{Zr}_x\text{O}_2$ thin films encapsulated by TiN electrodes that show linear dielectric (LD), ferroelectric (FE), and antiferroelectric (AFE) behavior. A wake-up (WU) effect is observed for AFE ZrO_2 , a phenomenon barely reported for pure zirconium oxide and AFE materials in general, correlated to the disappearance of the pinched hysteresis loop commonly observed for Zr-doped HfO_2 thin films. ESD and η are compared for FE, AFE, and LD samples at the same electrical field (3.5 MV/cm). As expected, ESD is higher for the FE sample (95 J/cm³), but η is ridiculously small ($\approx 55\%$), because of the opening of the FE hysteresis curve inducing high loss. Conversely, LD samples exhibit the highest efficiency (nearly 100%), at the expense of a lower ESD. AFE ZrO_2 thin film strikes a balance between FE and LD behavior, showing reduced losses compared to the FE sample but an ESD as high as 52 J/cm³ at 3.5 MV/cm. This value can be further increased up to 84 J/cm³ at a higher electrical field (4.0 MV/cm), with an η of 75%, among the highest values reported for fluorite-structured materials, offering promising perspectives for future optimization [3].



Current versus electric field measurements for pristine samples (dashed lines) and 10^3 cycles (straight lines) of (a) FE HZO (b) AFE ZrO_2 and their corresponding polarization versus electric field measurements of (c) FE HZO (d) AFE ZrO_2 . The observed change in current between pristine and 10^3 cycled samples correspond to the wake-up effect (WU), resulting in the switching current peaks shift over the voltage axis highlighted by the red arrows.


Acknowledgements:

This work was carried out on the NanoLyon technology platform and implemented inside the NanOx4EStor project, which has received funding under the Joint Call 2021 of the M-ERA.NET3, an ERA-NET Cofund supported by the European Union's Horizon 2020 research and innovation program under grant agreement No 958174. This work was supported by the Agence Nationale de la Recherche (ANR) under the contract ANR-22-MER3-0004-01.

References:

- [1] "Digitalisation and energy," Tech. Rep. (International Energy Agency (IEA), 2017).
- [2] J. P. B. Silva, K. C. Sekhar, H. Pan, J. L. MacManus-Driscoll, and M. Pereira, "Advances in dielectric thin films for energy storage applications, revealing the promise of group iv binary oxides," ACS Energy Letters 6, 2208–2217 (2021).
- [3] Grégoire Magagnin, Jordan Bouaziz, Martine Le Berre, Sara Gonzalez, Damien Deleruyelle, and Bertrand Vilquin, "Comparative performance of fluorite-structured materials for nanosupercapacitor applications", APL Mater. 12, 071124 (2024).

Oxidation and deoxidization process of semiconductors and metals

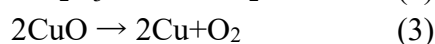
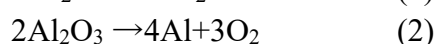
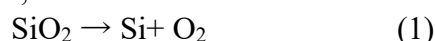
	<p>Prof. Kazuhiko Endo</p> <p>Institute of Fluid Science, Tohoku University</p>		
---	---	--	--

Abstract

Oxidation and deoxidization of Si, Al, and Cu oxides have been carried out in controlled low oxygen partial pressure atmosphere. The oxygen was evacuated to 10^{-28} atm by using an oxygen reduction system (ORS). It was experimentally demonstrated that the oxide of Si, Al, and Cu film was completely removed by exposure to such an environment¹. The proposed deoxidization reaction can be used as a new deoxidation and eventual surface cleaning technique.

Thermodynamics tells us that the deoxidization reaction of the metal is controlled by the temperature and oxygen partial pressure $p(O_2)$ in which the surface of the metal is exposed². If $p(O_2)$ is reduced below the equilibrium value at a certain temperature, the deoxidization reaction will proceed.

To deoxidize the oxidized materials without any degradation, we have developed a new technique not based on any chemicals. We used the deoxidization of materials through the reaction;



Thermodynamics tells us that the deoxidization reaction of the metal is controlled by the temperature and oxygen partial pressure $p(O_2)$ in which the surface of the metal is exposed. If $p(O_2)$ is reduced below the equilibrium value at a certain temperature, the deoxidization reaction will proceed. Thermodynamical equilibrium shows that the decomposition of the Cu oxide requires above 400°C in the conventional furnace, however, if we can reduce the $p(O_2)$ in the furnace below 10-15 atm, we will be able to decompose Cu oxide below 400°C, i. e. within the limited thermal budget of the interconnects.

To realize such reduction of oxygen partial pressure, we have developed a new oxygen reduction system (ORS) using a solid electrolyte tube. The solid electrolyte tube for the ORS was an yttria stabilized zirconia (YSZ). To apply a bias voltage to the YSZ, platinum electrodes were attached on both outer and inner surfaces of the YSZ tube. When an oxygen molecule hits the inner electrode, it will be immediately ionized. The ions are attracted to positively charged outer electrode, where a pair of them are recombined into one oxygen molecule and swept away. Thus, if we feed the process gases into the YSZ tube, $p(O_2)$ of the gases will be reduced during

the flow through the tube. We used the commercially available YSZ tube. The length of the tube was 250 mm. The external and internal diameters of the tube were 10 mm and 7 mm respectively. The YSZ tube was heated up to 600°C so that it could act as the solid electrolyte. The process gases were introduced into the tube through an electrically controlled mass flow controller. After flowing through the YSZ tube, the process gas with reduced oxygen pressure was introduced into the annealing apparatus. The process gas after flowing through the apparatus returned to the YSZ tube in order to regenerate the low oxygen pressure. The oxygen partial pressure was monitored by the oxygen sensor located at both inlet and outlet of the annealing apparatus.

The Cu samples used in this study were 100 nm-thick Cu films sputtered on a Si₃N₄ barrier dielectric film on a silicon substrate. The $p(\text{O}_2)$ of 10⁻¹⁵ atm, which was the minimum requirement of the Cu deoxidization below 400°C, was achieved immediately after the evacuation. Furthermore, the $p(\text{O}_2)$ of 10⁻²⁸ atm was successfully achieved after the 2 hours evacuation. Note that the evacuation speed can be improved by using a larger capacity ORS in the future.

The initial Cu film was covered with the native oxide, however, that was completely removed and pure Cu was revealed without using any chemicals and at the temperature as low as 200°C in the Ar gas flow with the $p(\text{O}_2)$ of 10⁻²⁸ atm. We also confirmed that the deoxidization did not occur at 150°C with the $p(\text{O}_2)$ of 10⁻²⁸ atm because the reaction condition was oxidation region.









In summary, by controlling thermodynamical reaction, oxygen in the metal and semiconductor films can be completely removed at the lower temperature under the extremely low oxygen ambient with no use of chemicals.

References

- 1 Kazuhiko Endo, Naoki Shirakawa, Yoshiyuki Yoshida, Shin-ichi Ikeda, Tetsuya Mino, Eishi Gofuku and Eiichi Suzuki, *Jpn. J. Appl. Phys.* 45 L393 (2006).
- 2 J.J. Lander and J. Morrison, *J. Appl. Phys.* 33, 2089 (1962).

Recent results of the MIMECHAS project on Al-steel welding

ELyT Global
Theme: Transportation
Scientific topic: Materials & Structure design

	B. Leflon ^{1, 2, 3, 4}		K. Suzuki ¹		S. Dancette ^{2,3}
	S. Tokita ¹		T. Chaise ⁴		C. Le Bourlot ³
	N. Mary ³		Y. Sato ¹		

Affiliation

1: Department of Materials Processing, Tohoku University, Sendai, Japan

2: ELyTMaX IRL3757, CNRS, Univ Lyon, INSA Lyon, Centrale Lyon, Université Claude Bernard Lyon 1, Tohoku University, Sendai, Japan

3: Univ Lyon, INSA Lyon, CNRS UMR5510, Laboratoire MATEIS, Villeurbanne, France



4: Univ Lyon, INSA Lyon, CNRS UMR5259, LaMCoS, Villeurbanne, France

Abstract

The MIMECHAS project investigates the formation, microstructure and mechanical properties of the brittle intermetallic compound (IMC) developing at the interface during aluminum-steel welding, and their consequences on the performance of the welded joints.

We report here recent results obtained on the link between process parameters, local thermal history and the growth of the IMC at the interface. These were obtained using a coupled experimental-numerical approach of instrumented welding and finite element (FE) simulations of the welding process, accompanied by detailed microstructural characterization of the IMC layer. The mechanical behavior of the resulting welds, with or without additional alloying elements in the welding pool, is explored by digital image correlation and FE analysis.

Metallization on Oxide Ceramics by Low Pressure Cold Spray and Its Deposition Mechanism Analyses

	<p>Prof. Kazuhiro OGAWA</p> <p>Tohoku University</p>		<p>Dr. Minjae YU, Dr. Hiroki SAITO, Prof. Yuji ICHIKAWA</p> <p>Tohoku University</p>
---	---	--	---

Abstract

Ceramic metallization is an essential element in power electronic modules. The most widely used ceramic metallization for power modules is direct-bonded copper (DBC) technology. However, the high pressure and operating temperature (1060 deg.C, close to the melting temperature of copper) result in oxidation and phase change of the metal. Therefore, this study applied low-pressure cold spray (LPCS) technology to overcome these shortcomings. It is possible to limit the oxidation and phase change of the materials.

LPCS technology has been widely applied to metal particles/metal substrates. However, the LPCS of metal particles on ceramic substrates have seldom been investigated. In addition, the mechanism of deposition of metal particles onto ceramic substrates was also unknown. Therefore, this study aims to successfully realize ceramic metallization using copper feedstock powders and demonstrate the deposition mechanism of metal particles onto ceramic substrates.

First, various composite powders and ceramic substrates were studied to realize the copper metallization of ceramics. It was able to successfully deposit copper using a copper/aluminum composite powder. The optimal ratio of composite powder was suggested in considering the copper content, thickness, and porosity of the coating. The highest coating thickness, copper content, and low porosity were obtained with 70% copper and 30% aluminum feedstock powder (Hereafter call Cu-70). Therefore, the optimal composite powder was used to study the effect of various ceramic substrates. Oxide ceramics can be deposited clearly with higher coating thickness than non-oxidized ceramics. However, non-oxide ceramic of silicon carbide even experienced delamination. Therefore, it is possible to suggest that oxide-based ceramics are more suitable for copper metallization.

The copper content of the coating directly affects the electrical and thermal conductivity. Therefore, as a next step, the operating parameters of LPCS that can increase the copper content were studied. Depending on the operating parameters of the LPCS, the thickness and copper content of the coatings changed significantly. The high copper content and thickness were manufactured at a higher gas pressure of 0.6 MPa and a short spray distance of 10 mm. Using optimizing the operating parameters on zirconia substrates, the coating thickness has been increased from as about 70 μm to 240 μm . In addition, the copper content could be increased

from a minimum of 38% to a maximum of 70%. The zirconia substrate showed higher thickness than the alumina substrate in the same oxide-based ceramic. This result suggests a possibility due to the high temperature of the zirconia substrate and oxygen mobility. Therefore, an important mechanism is assumed and suggested that the movement of oxygen on the ceramic substrate for the deposition of metal particles.

And then, various pre-treatments were performed that are increasing the copper content of the coating layer and improving its thickness. The bond coating is applied to realize pure copper deposition. Aluminum and Cu-70 bond coatings were applied, and both bond coatings are enabled to manufacture the pure copper coating on ceramic substrates. In addition, a method to increase the deposition efficiency through pre-treated substrates using a laser was studied. A high-thickness coating was obtained using a high-roughness laser texturing substrate. In addition, oxygen mobility was indirectly proved through laser pre-treatment (L)/laser pre-treatment with heat treatment (LH) which differs only in the oxygen content of the substrate. The LH substrate with a high oxygen content on the surface obtained a thicker coating, confirming that oxygen mobility from the ceramic substrate to the metal coating is significantly involved in the deposition.

As a result, copper was successfully coated using a copper and aluminum composite powder. The coating with best porosity, thickness, and copper content could be deposited using the Cu-70 composite powder. In addition, it is possible to realize the pure copper coating with the bond coating method. Unlike metal substrates, coatings on ceramic substrates had similar tensile strength regardless of the interface position using the micro-tensile test. The destruction of the native oxide film and the diffusion of oxygen are essential factors to determine the metallization deposition mechanism of ceramics using LPCS.

Finally, various studies were performed to understand the deposition behavior and mechanism of metals on ceramic substrates. Different adhesion strengths between the alumina substrate and the zirconia substrate were obtained by the adhesion strength test. Significantly different results were obtained for the after-fracture interface as well. The alumina substrate broken due to the lower impact strength was detected, which make decreased the adhesion strength. In addition, single aluminum and copper particles with varied contact lengths on alumina and zirconia substrates were also observed at the microscale. A longer contact length was obtained with aluminum, which is easier to plastically deform. And lower contact lengths were obtained on alumina substrates with a lower roughness than particle than on the smooth surface of zirconia substrate. It has been confirmed that the surface roughness of ceramics is an important factor for metal particle deposition. In addition, it was confirmed that the deposition behaviors of metal substrates and ceramic substrates are different using the micro-tensile test. Metal substrates have a strong tensile strength at the particle edges, whereas ceramic substrates have similar tensile strengths at the center and edges of particle. Therefore, aluminum has a higher tensile strength than copper, which supports the deposition of copper particles in the composite powder. In addition, the deposition mechanism of the oxygen mobility of metal particles from the ceramic substrate was directly proved by TEM analysis. A gap was detected where the native oxide film remained thick without being broken. Furthermore, the position where the native oxide film was completely broken was deposited clearly. Oxygen mobility was detected at the new surface of the clearly deposited metal using TEM-EDS mapping. This suggested that the native oxide film was broken, and oxygen mobility occurred on the new surface, leading to strong adhesion. As a result, it was proved that the new surface of metal particle and oxygen mobility are the most important factors in the deposition of metal particles on oxide ceramic substrate.

Insights into Solid Lubrication Processes of DLC Films thanks to Analytical Tribology

ELyT Global Theme: Transportation or Energy Scientific topic: Surfaces & Interfaces



Antoine NORMANT^{1,2}, Jules GALIPAUD^{1,3}, Frédéric DUBREUIL¹, Julien FONTAINE¹

1. LTDS UMR 5513, CNRS, Ecole Centrale de Lyon, France
2. Now at: LaMCoS, UMR 5259, CNRS, INSA Lyon, France
3. MatéIS, UMR 5510, CNRS, INSA Lyon, France

Abstract




Diamond-Like Carbon coatings may behave as very good solid lubricants, providing a good combination of tribological environment and coating composition is ensured. For instance, highly hydrogenated amorphous carbon (a-C:H) films may lead to super low friction regime ($\mu < 0.01$) under ultra-high vacuum, at least for a limited time. What are the tribological phenomena that allow for such performance, and what brings an end to this unique regime?

To answer such questions, a traditional approach consists in performing some surface analysis after the experiments, inside and outside the wear tracks. These analyses are frequently morphological, structural or chemical, sometimes mechanical. While such information is paramount for the understanding of the surface degradations during sliding, it doesn't provide information about the respective roles of these degradation on the evolution of the tribological response of the contact.

In this work, we use a high-resolution environment-controlled tribometer, based on a six axes force sensor, to probe the tribological response of a steel pin / a-C:H film contact, either by crossing existing wear tracks or by shifting the tracks to slide on pristine surfaces. This original approach helps understanding the respective role of surface modifications on the a-C:H coated flat or on the facing steel pin on the achievement of superlow friction. These experiments are combined with more traditional analytical means, like *in situ* XPS, AES and REELS analyses or *ex situ* SEM or AFM observations. The growth of a carbon-rich tribofilm on the steel counterpart appears necessary, but not sufficient to reach superlow friction. Changes on the topography and chemistry of the a-C:H film seems also paramount, with a smoothening of the a-C:H asperities and an increase of the sp^2 Carbon content. The respective role of these phenomena on the solid lubrication process of a-C:H film will be discussed.

Multiscale Analysis of the Rubber/Ice Tribological Interface

ELyT Global
Theme (Transportation)
Scientific topic (Surfaces & Interfaces)

	PhD Student Anderson DALAVALÉ KAISER PINTO		CNRS Director of Research LTDS Juliette CAYER- BARRIOZ		Prof ECL Denis MAZUYER
---	---	---	---	---	--------------------------------------

Abstract

According to the U.S. Department of Transportation, 24 percent of annual car accidents are attributed to snow or ice on roads, encompassing both minor and severe collisions. Additionally, the International Union for Conservation of Nature reported that tires accounted for 28 percent of microplastic pollution in oceans as of 2017, making them the second-largest source of such pollutants.

This study addresses two critical challenges - enhancing road safety on icy surfaces and mitigating environmental pollution - by investigating the interfacial friction response of ice/rubber contacts under a broad range of environmental conditions. Experiments were conducted at temperatures as low as -28°C and sliding velocities ranging from 50 µm/s to 1 m/s. Rubber samples, provided by Michelin, varied in composition, surface topography, and mechanical properties. The ice used in the experiments was homogeneous, transparent, and prepared through a controlled machining and thermalization process.

A novel in-situ contact area measurement methodology was developed to capture the static and dynamic behavior of the ice-rubber interface during mechanical loading, unloading, and sliding. By combining in-situ visualization of contact areas with friction force analysis, the study elucidated the complex interplay between adhesion, viscoelastic, and thermal effects in governing frictional behavior. These mechanisms were examined as functions of sliding velocity and temperature, providing insights into the dynamics of the ice-rubber interface in real-time.

Building on the foundational work of Schallamach and later developments by Chernyak and Leonov, a friction model was proposed to account for molecular-level interactions. This model incorporates the time-temperature dependence of the formation and rupture of molecular junctions at the rubber-ice interface, offering a comprehensive framework for understanding and predicting frictional performance under diverse conditions.

Mechano-Chemically-activated Tribofilm Growth at Nanoscale

**ELyT Global
MeCaT**

	<p>Dr. Shaoli JIANG</p> <p>Department of Mechanical Systems Engineering, Tohoku University, Sendai 980-8579, Japan</p>		<p>Dr. Motoyuki MURASHIMA</p> <p>Department of Mechanical Systems Engineering, Tohoku University, Sendai 980-8579, Japan</p>
	<p>Prof. Jean Michel MARTIN</p> <p>Ecole Centrale de Lyon CNRS LTDS UMR5513</p> <p>69130 Ecully, France</p>		<p>Dr. Maria Isabel DE BARROS BOUCHET</p> <p>Ecole Centrale de Lyon CNRS LTDS UMR5513</p> <p>69130 Ecully, France</p>

Abstract

In general, the activation of chemical reactions requires energy, which is typically provided by heat, light or electrical potential. When mechanical contact generates a stress field at the interface between two surfaces, certain mechanically induced chemical reactions are initiated or accelerated. In the field of tribology, mechanochemical effects have been used to generate functional layers (known as tribofilms) on the surface of mechanical components, reducing wear and friction. In most tribological research experiments, these reactions are activated simultaneously at the tips of numerous microscopic asperities (surface roughness), where locally distributed tribofilms generate and eventually get mixed into a uniform layer. As a result, tribofilms form rapidly on uncertain areas under unquantified pressures, making it impossible to independently interpret the tribofilm growth kinetics. Additionally, most studies so far only show finally formed chemicals of tribofilm through post-test analysis while involved intermediate chemical transformation is largely unknown.

As the most successful antiwear additive ever invented, zinc dialkyldithiophosphate (ZDDP) is reported to decompose with physicochemical pathways, leading to protective tribofilm. However, there is no information on the evolution of their compositions and concentrations, as well as distribution within tribofilm. In this work, by mimicking sliding nanocontacts using atomic force microscopy (AFM), ZDDP tribofilms formation process was observed *in lubro*, starting with some tiny platelets that grow in height and further more platelet-like feature

generation which is in agreement with the studies performed in macroscopic friction tests.

Subsequently, numerous additional characterizations were performed on the tribofilms developed using this approach. ToF-SIMS analysis demonstrates that developed tribofilms consist primarily of phosphate-based structures generated by mechanochemical reaction. High-resolution TEM observations coupled with chemical and structural analyses further reveal that its formation follows the hard and soft acid base (HSAB) principle. These findings offer valuable insights into the mechanisms governing antiwear tribofilms formation. This *in lubro* nanoscale approach is also highly relevant for studying potential interactions/competition between ZDDP and other surface additives affecting tribofilm formation.

**Friday,
February 21st**

Morning

Introduction of Integrated Flow Science and recent activities of the Institute of Fluid Science, IFS, Tohoku University

	<p>Prof. Director Kaoru MARUTA IFS, Tohoku University</p>		<p>Prof. Tetsuya UCHIMOTO IFS, Tohoku University</p>
---	--	--	--

Abstract

Institute of Fluid Science, IFS, Tohoku University, founded originally in 1943, is dedicated to advancing knowledge in fluid science through cutting-edge research and international collaboration. With a history rooted in innovation, we have expanded our research scope to include various kinds of fluid and transport phenomena, while fostering international partnerships with leading organizations worldwide.

Since 2022, our institute has embraced the new concept of "Integrated Flow Science," aiming to contribute to solving challenges in human activities through fundamental and applicational research in a wide range of transport phenomena. By leveraging our strengths in fluid dynamics, we employ supercomputing, advanced experimental techniques, and molecular and atomic simulations to address critical issues in areas such as energy and the environment, biomedical engineering, and aerospace applications.

In this context, we are pleased to introduce a new project launched under the Singapore government's initiative to promote decarbonization using ammonia as a fuel. This three-year program, starting in October 2024, initially focuses on combustion research utilizing ammonia as a clean energy source. Following this foundational phase, the project aims to broaden its scope to address critical areas such as the production of clean ammonia fuel, its transportation and storage, research on ammonia-resistant materials, and innovative applications, including combustion technologies. Ultimately, this initiative seeks to establish an international supply chain for fuel ammonia, contributing significantly to global decarbonization efforts.

We are excited about the opportunities this endeavor presents and look forward to collaborating with you to drive sustainable energy solutions forward.

Multi-scale study on cavitating flow with liquid-vapor phase change

ELyT Global
**Modeling of Cavitation
Water, Cryogenic Fluids**





Abstract

Recently, a more accurate prediction technique of cavitating flows has been required due to a further demand for designing smaller turbopumps with high-speed rotation, whose working liquids are not only water but also cryogenic fluids such as liquid hydrogen as one of clean energy sources. However, particularly for liquid hydrogen, an accurate prediction of the cavitating flows is currently difficult due to fewer knowledge on the liquid-vapor phase change as well as fewer experimental data. In addition, it is essentially necessary to understand the multi-scale structure of cavitation with liquid-vapor phase change for developing more appropriate cavitation model implemented in Computational Fluid Dynamics (CFD) solvers because cavitation phenomenon includes various elementary processes whose scales are variant, and particularly, cryogenic cavitation inception may occur on a molecular scale like homogeneous bubble nucleation. In this study, we have firstly constructed a multi-scale cavitation model called as Multi-Process (MP) model, in which the main elementary processes of cavitation such as bubble expansion/shrinkage as a macroscopic scale and bubble inception or evaporation as a microscopic scale can be simultaneously considered. In addition, for clarification of the microscopic processes, i.e., bubble inception and evaporation, Density Functional Theory (DFT) and Molecular Dynamics (MD) simulations were applied particularly presuming liquid hydrogen. Finally, we are going to summarize both the macroscopic and microscopic acknowledgment into the MP model applied in a high-accuracy turbulent CFD, i.e., Wall-Resolved Large Eddy Simulation (WRLES).

Solid particle impact on CO₂ absorption among phytoplankton blooms.

ELyT Global

Theme : Ocean, chemical engineering
Scientific topic : CO₂ captation, phytoplankton, solid particles.

	<p>Dr S. Simoëns, CNRS Research Director</p> <p>LMFA, ECL, INSA, UCB Lyon I, UMR CNRS 5509</p>	 	<p>Dr. M. El Hajem, Pr. I. Vinkovic, C. Lozet, Doctorant,</p> <p>LMFA, ECL, INSA, UCB Lyon I, UMR CNRS 5509</p>
---	---	---	--

Abstract

Here we are interested in the evaluation of the absorption of atmospheric CO₂ in the oceans. We thus distinguish two types of absorption: 1) biological absorption (via phytoplankton), 2) passive absorption (dissolution then transport to the shallows for deposition). Among the factors that modulates this latter absorption, there are the environment in the presence of phytoplankton, solid particles, turbulence, etc. All these factors influence the basic absorption coefficient (CO₂ at atmospheric pressure towards the ocean). For example, the proliferation (blooms) of phytoplankton is seasonal and can locally and cyclically modify the properties of the water (oceans, lakes) and consequently the local currents and other turbulences which are the drivers of the dispersion (transport) of dissolved CO₂ towards the shallows. In particular, the rheology of the surrounding water can be strongly modified and resemble a non-Newtonian environment. In addition, associated with these proliferations are the wind transport of solid particles (particle flight event from deserts) or water runoff which, among other things, feeds the oceans with various

chemical compounds and in particular “feeds” phytoplankton allowing them exponential growth. The impact of all these phenomena in the evaluation of the transport coefficients of dissolved CO₂ in the oceans or lakes is very poorly understood and must be studied.

To account the non-Newtonian properties associated (elasticity, viscosity) with the presence of phytoplankton, polymers at low concentrations can be used. Many types of polymers are used in fields concerning biochemistry, process engineering, etc. Solid particles due to wind or runoff events are of different nature and of very variable diameters. For the studies of interest and related to the transport and mixing of dissolved CO₂, we use precise ranges of diameters and density corresponding to a wind problem.

Despite initial experimental studies (1) and a fairly old theory (2), it remains quite difficult to study non-Newtonian turbulent flows and few complete and characteristic experiments allow the theory to progress (3). Similarly, experiments on the transport of solid particles in non-Newtonian turbulent flows are very rare. We will focus here on shear-thinning non Newtonian fluids. A first problem lies in the separation of the so-called "viscoelasticity" effects from those called "shear thinning" in order to know which one is the main responsible for drag reductions for example.

The LMFA (PhD T. Lacassagne, 2018) highlighted the influence of the non-Newtonian character on the transport and turbulent mixing of dissolved CO₂ (4). The oscillating grid turbulence used is small (60cm*60cm*100cm). A grid is arranged horizontally and allows the generation of stationary turbulence. We are now inspecting the presence of solid particles to perform the same measurements and analyses (PhD C. Lozet, 2025-2027). The measurements are carried out by VIP (Particle Image Velocimetry) or PTV (Particle Tracking Velocimetry) for the velocity field information and PLIF (Planar Laser Induced Fluorescence) for the concentration field of dissolved CO₂. Influence of solid particles on CO₂ absorption is the final objective.

[1] B. A. Toms, Some observation on the ow of linear polymer solutions through straight tubes at large Reynolds numbers (J.G. Oldroyd, Scheveningen, 1948) pp. 135-141.

[2] J. L. Lumley, Drag Reduction by Additives, Annual Review of Fluid Mechanics 1, 367 (1969).

[3] M. Tabor and P. G. d. Gennes, A Cascade Theory of Drag Reduction, EPL (Europhysics Letters) 2, 519, 1986.

[4] T. Lacassagne, S. Simoëns, M. ElHajem, J.Y. Champagne, Oscillating grid generating turbulence near gas-liquid interfaces in shear-thinning dilute polymer solutions, Phys. Rev. Fluids 5, 033301, 31 March, 2020

Robust Multi-objective optimization schemes: applications for shape design of mechanical parts

ELyT Global Project ELyT lab : R7 – Robust Multi Objective optimization design approaches

	Koji SHIMOYAMA¹		Frédéric GILLOT²
	Hiroshi, SUIITO³		Sébastien BESSET²
			Thanasak, WANGLOMKLANG²

¹Department of Mechanical Engineering, Kyushu University, Japan

²Ecole Centrale de Lyon, LTDS DySCo Team, Lyon, France

³Advanced Institute for Materials Research, Mathematical Science Group, Tohoku University, Japan

Abstract

Framework of our collaborative research studies concerns robust shape optimization of structures and systems under extremes conditions. Load involves in such conditions usually leads to non-linear behavior of structures, making figure of merits computationally costly and without accessible derivatives.

As an applicative example, we have worked on a disc-pad system exhibiting vibro-acoustic properties arising from friction-induced vibration, commonly known as squeal

noise. We are now designing cavities shapes w.r.t. inner noise level considerations, like what can be considered for cabin design of modern airplanes (see fig. 1.).

The complex nature of those problems demands an efficient optimization strategy considering the computation cost. It is addressed through defining the expensive evaluation with a meta-model and using a dedicated Efficient Global Optimization (EGO)-like search algorithms. The multi-objective definition of the optimization results in pareto-optimal solutions obtained through genetic algorithm for the considered shape parameters.

1. Achieved results

The deterministic optimization loop has been addressed during Pradeep Mohanasundaram Ph.D. as a double diploma student (ECL / TU – 2017-2021). Uncertainties quantification within the optimization loop has been addressed by Achille Jacquemond Ph.D., (ECL – 2021-2024). Results have been presented in journal papers [1,2]. Achille has stayed three months within Pr. Shimoyama Lab. under a JSPS Summer Grant (June-August 2022) to develop a noisy Kriging for robustness criteria building. He has been awarded a JSPS Short Term Post Doc. for one year (May 2023 – April 2024) within Pr. Obayashi Laboratory to develop the LARS-PCE meta-model.

More recently Thanasak Wanglomklang has started his Ph.D. since October 2023 to look into the use of radial basis functions kernels inside the optimization loop, and is starting a collaboration with Pr. Suito team. Pr. Gillot has been welcomed at the IRL at T.U. ('CNRS Delegation') for one year, Sept. 2023 to Aug. 2024.

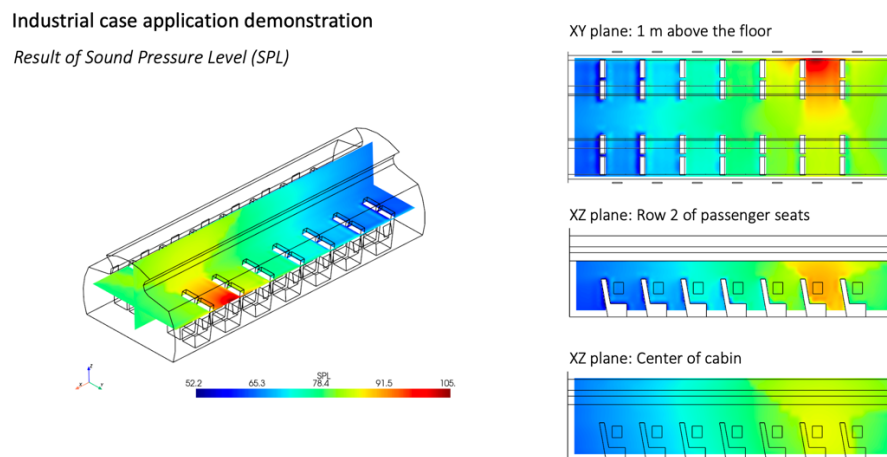









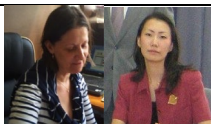



Figure 1: Sound Pressure Level of inner A320 Airbus airplane cabin

References :

- [1] Achille Jacquemond, , Frédéric Gillot, Sébastien Besset, and Koji Shimoyama. "Noisy Kriging for robust shape optimization of mechanical systems with a nonlinear and gradient-free expensive black-box figure of merit". *European Journal of Mechanics - A/Solids* 111 (2025): 105567.
- [2] Achille Jacquemond, , Frédéric Gillot, Sébastien Besset, and Koji Shimoyama. " Pareto optimal robust design combining isogeometric analysis and sparse polynomial chaos: brake squeal case study". *Archive of Applied Mechanics – accepted 11/2024*.

EBl Induced Ductility of Brittle 3D-Printed Short Fiber Reinforced PA

ELyT Global
Effects of EBl to Polymers & its Composites
EBl Induced Adhesive force of CF/Polymers

      	<p>Helmut Takahiro UCHIDA, Kousuke SAGAWA, Masae KANDA*, Eiichi MIURA**, Michael C. Faudree***, Hideki KIMURA, Yoshitake Nishi Tokai University, 〒259-1292, 4-1-1, Kitakaname, Hiratsuka, Kanagawa, Japan. * Chubu Univ., ** KISTEC, ***Tokyo City Univ.</p>	   	<p>Michelle Salvia¹, Kaori Yuse², Daniel Gyomar², Jean-Yves CAVAILLE² ¹ Ecole Centrale de Lyon, Ecully Cedex 69134, France, ² INSA Lyon, Bât. B. Pascal, 5^e étage, 7, Avenue Jean Capelle, 69621 Villeurbanne cedex FRANCE</p>
---	--	---	---

Abstract

Since 1998, our target of the projects has been the rising the international active collaborations for Research for constructed and smart materials with original concepts. Excellent results was getting PhD (INSA Lyon) of a (Tokai Univ.) M. Kanda, as well as following papers collaborated with three Research Alliances. Recent topics (2024) will be introduced. It is a serious problem that 3D-SCFRPA66 (short carbon fiber reinforced polyamide66 shaped by 3D-printing) articles are brittle for practical usages. To improve the brittleness, HLEBI (homogeneous low potential electron beam irradiation) was performed to both sides of 3D-SCFRPA66 samples. As a results, ϵ_{ts} (the ductility was achieved by the parameters: strain at tensile strength corresponding to homogeneous deformation, ϵ_f (fracture strain), and E_{hd} (resistance energy of homogeneous deformation). That is, the slight HLEBI dose to both sides of 3D-SCFRPA66 samples increased ϵ_{ts} , ϵ_f , and E_{hd} , 8, 9 and 5 times higher than untreated, respectively. Improvement in ductility can be explained by lone pair electrons, dangling bond generation, shortening and relaxation of the polymeric chains by the HLEBI.

Based on the collaboration with ECL (M. Salvia), the CFRPs (fiber reinforced polymer) have been investigated. They are ①:Novel Treatment for 3D Printed Short Carbon Fiber Reinforced Polyamide (3D-SCFRPA66) of Homogeneous Low Potential Electron Beam Irradiation (HLEBI) on Tensile Properties, E Miura, H-T. Uchida, T. Okazaki, K. Sagawa, M. C. Faudree, M. Salvia, H. Kimura, Y. Nishi, *Polymers*, accepted 2024 Nov.27th. ②:[HLEBI \(Homogeneous Low Potential Electron Beam Irradiation\) Induced Tensile Elongation of 3D Printed Short Carbon Fiber Reinforced Polyamide \(3D-SCFRPA66\)](#), E. Miura, H. T. Uchida, T. Okazaki, K. Sagawa, F. Satoh, H. Irie, M. C. Faudree, M. Salvia, H. Kimura, Y. Nishi, *Materials Forum*, in press.2024 7th International Conference on Advanced Composite Material (2024) Aug. ③:[Increasing Bending Strength of Polycarbonate Reinforced by Carbon Fiber Irradiated by Electron Beam](#) :Y. Nishi, N. Tsuyuki, H. T. Uchida, M. C. Faudree, K. Sagawa, M. Kanda, Y. Matsumura, M. Salvia, H. Kimura, *Polymer <Special Issue Processing, Characterization and Engineering Application of Fiber-Reinforced Thermoplastic Polymer Composites>* 15(22) 4350-4364 (2023), ④: [A Novel Nickel-Plated Carbon Fiber Insert in Aluminum Joints with Thermoplastic ABS Polymer or Stainless Steel](#), Y. Nishi, K. Sagawa, M. C. Faudree, H. T. Uchida, M. Kanda, S. Kaneko, M. Salvia, Y. Matsumura, H. Kimura, *Materials* 16(17) 5777-5777 (2023), ⑤ : [Improvements of Strength of Layered Polypropylene Reinforced by Carbon Fiber by its Sizing Film and Electron Beam under Protective Nitrogen Gas Atmosphere](#): Y. Nishi, S. Kitagawa, M. C. Faudree, H. T. Uchida, M. Kanda, S. Takase, S. Kaneko, T. Endo, A. Tonegawa, M. Salvia & H. Kimura: *Suzuki Carbon Book* (©,© Springer Nature Singapore Pte Ltd.2021, ISBN978-981-15-7609-6 & -7610-2 (eBook) <https://doi.org/10.1007/978-981-15-7610-2>, Chapter 12, pp. 279-302, ⑥ : [Advances in Titanium-Polymer Hybrid Joint by Carbon Fiber-Plug Insert: Current Status and Review](#), M. C. Faudree, H. T. Uchida, H. Kimura, S. Kaneko, M. Salvia, Y. Nishi, *Materials <Special Issue Organic Matrix Composites and Multifunctional Materials.15-3220-PP1-19.>* 15 (9)(3220) pp1-19 (2022), ⑦ : [A Novel Joint of 18-8 Stainless Steel and Aluminam by Partial Welding Process to Ni-Plated Carbon fiber Junction](#): M. Tomozawa, M. C. Faudree, D. Kitahara, S. Takase, Y. Matsumura, I. Jimbo, M. Salvia & Y. Nishi, *Maters. Trans.* 61, 12 (2020) pp.2292-2301.⑧: [A New Process of Thermoplastic PP Reinforced by Interlayered Activated CF treated by EBl](#)

under nitrogen gas atmosphere with Oxygen prior to Assembly and Hot-press, S. Kitagawa, H. Kimura, H. T. Uchida, M. C. Faudree, A. Tonegawa, S. Kaneko, M. Salvia, Y. Nishi; *Mater. Trans.* 60, 4 (2019) 587-592, ⑨: Tensile strength of PP Reinforced by CF Covered with and without Sizing Epoxy Film, S. Kitagawa, H. Kimura, S. Takase, N. Tsuyuki, D. Kitahara, A. Takahashi, M. C. Faudree, H. T. Uchida, A. Tonegawa, M. Kanda, N. Inoue, S. Kaneko, T. Endo, M. Salvia, Y. Nishi; *Trans. Materials Research Society of Japan* (2018) June, 125-128, ⑩: Enhanced Tensile Strength of Ti/PC Joint Connected by EB Activated Cross-Weave CF Cloth Insert (H. Hasegawa, M. C. Faudree, Y. Enomoto, S. Takase, H. Kimura, A. Tonegawa, Y. Matsumura, I. Jimbo, M. Salvia and Y. Nishi , *Mater. Trans.* 58(11) (2017) 1606-1615, ⑪: Improvement of Bending Modulus and Impact Value of Injection-Molded Short CF Reinforced PEEK with HLEBI (Y. Nishi, R. Ourahmoune, M. Kanda, J.H. Quan, M.C. Faudree and M. Salvia; *Mater. Trans.*, **55** (8) (2014) 1304-1310, ⑫: Effects of EBI on Elasticity of CFRTPE (CF/PEEK), (H. TAKEI, M. Salvia, A. Vautrin, A. Tonegawa, Y. Nishi; *Mater. Trans.* **52** (4) 2011 pp734-739), ⑬: Effects of EBI on Impact Value of Novolak-Type Phenol CFRTPE (Y. Nishi, H. Takei, K. Iwata, M. Salvia, A. Vautrin, *Mater. Trans.* 51 (12) (2010) 2259-2265, and ⑭: Effects of EBI on Impact Value of CFRTPEEK (Y. Nishi, H. Takei, K. Iwata, M. Salvia, A. Vautrin; *Mater. Trans.* **50** (12) (2009) 2826-2832.

Based on the collaboration with LGEF, INSA de Lyon (D. Guyomar & K. Yuse), the Sensor and Actuators have been investigated and constructed with ① Effect of 100 keV Class Electron Beam Irradiation on Impact Fatigue Behavior of PZT Ceramics (N. Tsuyuki, A. Takahashi, S. Takase, D. Kitahara, M. Kanda, N. Inoue, K. Yuse, D. Guyomar, A. Tonegawa, Y. Matsumura and Y. Nishi; *Materials Trans.* Vol.59, (3)(2018) pp.450-455, ② An Improved H₂-Gas Pressure Operated LaNi₅ Powder-Dispersed PU/Ti 2-Layer Actuator with Reversible Giant and Rapid Expansion by Hydrogenation (Y. Nishi, J. Ohkawa, M. C. Faudree, M. Kanda, K. Yuse, D. Guyomar, H. H. Uchida; *Materials Transactions*, Vol.59 No.01 (2018) pp.129-135), ③ Improvement of Electric Field Induced Compressive Electrostriction of PU Composites Film Homogeneously Dispersed with Carbon Nanoparticles, (M. Kanda, K. Yuse, B. Guiffard, L. Lebrun, Y. Nishi, D. Guyomar; *Materials Transactions*, Vol.56 No.12 (2015) pp.2029-2033.), ④ Actuation abilities of multiphase electroactive polymeric systems, (M. Lallart, J.-F. Capsal, A. K. Mossi Idrissa, J. Galigneau, M. Kanda, D. Guyomar; *Journal of Applied Physics*, Vol.112 (2012) 094108), ⑤ Solidification Thickness Dependent Electrostriction of PU Films (M. Kanda, K. Yuse, B. Guiffard, L. Lebrun, Y. Nishi, D. Guyomar; *Materials Transactions*, Vol.53 (2012) pp1806-1809), ⑥ Modeling of thickness effect and polarization saturation in electrostrictive polymers, (M. Lallart, J.-F. Capsal, M. Kanda, J. Galigneau, D. Guyomar, K. Yuse, B. Guiffard: *Sensors and Actuators B: Chemical*, Vol.171-172 (2012) pp739-746), ⑦ The compressive electrical field electrostrictive coefficient M₃₃ of electroactive polymer composites and its saturation versus electrical field, polymer thickness, frequency and fillers, (D. Guyomar, P.-J. Cottinet, L. Lebrun, C. Putson, K. Yuse, M. Kanda, Y. Nishi; *Polym. Adv. Technol.* (2011) DOI 10.1002/pat.1993), ⑧ Thickness effect on electrostrictive PU strain performances: A three-layer model, (D. Guyomar, K. Yuse, M. Kanda , *Sensors and Actuators A*, Vol.168 (2011) pp307-312.), ⑨ Development of large-strain and low-powered electro-active polymers (EAPs) using conductive fillers, (K. Yuse, D. Guyomar, M. Kanda, L. Seveyrat, B. Guiffard: *Sensors and Actuators A*, Vol.165 (2011) pp147-154.), ⑩ Focus on the electrical field-induced strain of electroactive polymers and the observed saturation, (D. Guyomar, K. Yuse, P.-J. Cottinet, M. Kanda, L. Lebrun, *J. Applied Physics*, Vol.108 (2010) 114910.), ⑪ Reversible Bending Motion of Unimorph Composites Driven by Combining LaNi₅ Alloy Powders Dispersed PU and Thin Supporting Cu Sheet under Partial Hydrogen Gas Pressure, (J. Okawa, M. Kanda, K. Yuse, H.H. Uchida, D. Guyomar, Y. Nishi , *Materials Transactions* Vol.51 (2010) pp994-1001.), and ⑫ Giant Bending Strain of Reversible Motion of Uni-Morph Soft Mover Composites Driven by Hydrogen Storage Alloy Powders Dispersed in PU Sheet, (Y. Nishi, S. Ohkawa, M. Kanda, A. Shimazu, R. Suenaga, Y. Ebihara, D. Kubo, H.H. Uchida, K. Yuse, D. Guyomar; *Materials Transactions*, Vol.50 (2009) pp2460-2465).

Based on the collaboration with MATEIS, INSA de Lyon (J-Y Cavaille), the Adhesion and strengthening of polymers induced by EBI process have been investigated and constructed with ① Adhesion of PE/PET Laminated Sheets by HLEBI Prior to Assembly and Hot-Press above Melting Point, (S. Takase, H. T. Uchida, A. Yagi, M. Kanda, O. Lame, J.-Y. Cavaille, Y. Matsumura, Y. Nishi; *Materials Transactions*, Vol.58 No.07 (2017) pp.1055-1062), ② Effects of HLEBI on Adhesive Force of Peeling Resistance of Laminated Sheet with PE and Austenitic 18-8 Stainless Steels (C. Kubo, M. Kanda, O. Lame, J.-Y. Cavaille, Y. Nishi; *Materials Transactions*, 57(3) (2016) 373-378), ③ Effects of HLEBI on Brazilian Bending Strength of Liquid Quenched Ten Mega Molecular Weight-Polyethylene (TMMW-PE) (Y. Nishi, M. Kanda, K. Shiraishi, S. Ishii, M. Uyama, S. Inui, M. C. Faudree, O. Lame and J.-Y. Cavaille, 2016Sept26th-Zaoh-ELYT WS abstract). ④ Evaluation of the Tensile Strength of EB Irradiated Powdered Ultra High Molecular Weight-Polyethylene (UHMWPE) Prior to Sintering (M. Kanda, T. Deplancke, O. Lame, Y. Nishi and J.-Y. Cavaille, *Materials Transactions*, 56 (9) (2015) 1505-1508), ⑤ High Electric Conductive PMMA Composites without Impact Value Decay by Dispersion of Cu Powder, (Y. Nishi, Y. Ebihara, N. Kunikyoh, M. Kanda, K. Iwata, K. Yuse, B. Guiffard, L. Lebrun, D. Guyomar, *Materials Transactions*, Vol.51 (2010) pp1437-1442.), and ⑥: Impact Value of High Electric Conductive ABS Composites with Cu Powder Dispersion Prepared by Solution-Cast Method, (Y. Nishi, N. Kunikyoh, M. Kanda, L. Lebrun, D. Guyomar; *Materials Transactions*, Vol.51 (2010) pp165-170).

Future contribution to J-F Collaboration: Our Research alliances were constructed with Tokai U. < A. Prof. Uchida (Hydrogen energy, EB-irradiation strengthening short fiber polymers prepared by 3D-printing and polymer adhesion), Prof. Kimura & A. Prof. Sagawa (Solar car & FRTP), KISTEC (Doctoral student. E. Miura) and Chubu University <A. Prof. Masae Kanda, PhD (Direct current Superconducting system, airplane-electrification) .

Sensor-Less Structural Health Monitoring using Semi-Active Controlled Piezoelectric Transducer

ELyT Global Theme (Energy) Scientific topic (Materials & Structure design)

	<p>Dr. Yushin HARA</p>		<p>Mr. Tianyi TANG</p>		<p>Prof. Kanjuro MAKIHARA</p>
--	-----------------------------------	--	-----------------------------------	--	--

Abstract

In-situ structural health monitoring (SHM) for large infrastructures has been attracted to achieve an economical and safe society. In-situ SHM uses three devices: actuators (signal generators), sensors (receivers), and power supplies. SHM could only be performed by carrying large equipment to the site and setting it up. The installation cost of these devices impedes the in-situ SHM. This study aims to solve and reduce this cost. Piezoelectric materials have an energy conversion property from mechanical energy to electrical energy. Based on this property, the piezoelectric material has been used for vibration excitation, vibration sensing, and vibration energy harvesting individually. These three applications correspond to the three required devices in the in-situ SHM. If three individual piezoelectric transducers are able to connect to the structure, the in-situ SHM is available without three large-scale equipment. However, three transducers are necessary.

This study proposes a multifunctional piezoelectric transducer for in-situ SHM. A single piezoelectric transducer is performed as an actuator and a sensor functions. Due to this study, the number of piezoelectric transducers required for SHM can be reduced from three to two. The piezoelectric transducer generates a voltage proportional to the deformation of the transducer and electrical charge. The charge inflows from an outer actuator controller to the transducer. The deformation of the piezoelectric transducer depends on structural vibrations. If only deformation information can be extracted from the voltage information, a piezoelectric transducer that functions as an actuator can be given a new sensor function. We paid attention to the dynamics of the outer actuator controller. We proposed a method to remove charge information from the voltage by taking advantage of the prior information that the controller generates for the charge on the square wave. The proposed method was validated via the two-degree-of-freedom vibrating structure equipped with the single piezoelectric transducer.

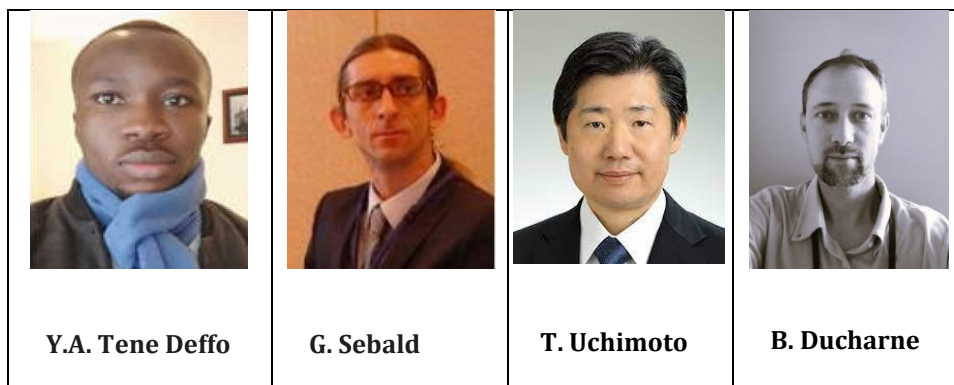
NDT based on the magnetization mechanisms:

last progress in the frame of BENTO.

(Nonlinear and dynamic micromagnetic Behavior modeling and characterization for Non-Destructive Testing techniques optimization).

ELyT Global

**Joint presentation: focus on the optical microscopy
Kerr-effect incremental permeability**



Abstract

This study presents an innovative approach to characterizing magnetic properties near grain boundaries in grain-oriented (GO) electrical steel, an essential material for energy-efficient transformers and motors. While GO electrical steel exhibits superior magnetic performance along the rolling direction, the influence of grain boundaries on magnetic behavior remains underexplored. This work addresses the challenge by combining Magnetic Incremental Permeability (MIP) measurements with a Magneto-Optical (MO) detection system to achieve high spatial resolution.

Traditional MIP setups utilize flat coils for excitation, limiting spatial resolution to millimeter scales. In contrast, this study replaces the detection coil with a Bismuth-substituted iron garnet film, employing the Faraday effect to achieve spatial resolution at the micrometer scale, determined by the laser diameter. The integrated system allows precise mapping of magnetic behaviors at grain boundaries, with the optical subsystem analyzing polarization changes in light reflected from the sample.

Experiments were conducted on GO electrical steel samples featuring large grains. The MIP butterfly loop was measured across a 2D scanning area, and parameters such as peak-to-peak and maximum incremental permeability values were extracted. The results demonstrate a clear correlation between the permeability distribution and grain boundary locations. The system effectively identifies grain boundaries, validating its ability to characterize localized magnetic properties with high sensitivity.

This work establishes a foundation for optimizing the microstructure of electrical steel laminations by providing a deeper understanding of grain boundary effects. Future research will focus on improving the system's sensitivity and extending the study to various grain boundary orientations relative to the rolling direction and applied magnetic field. The insights gained could significantly enhance the design and performance of GO electrical steel, contributing to energy savings in key industrial applications.

Recent papers (less than two years) in the Frame of BENTO collaboration:

[1] Diguët, G., Ducharne, B., El Hog, S., Kato, F., Koibuchi, H., Uchimoto, T. and Diep, H.T., 2024. Monte Carlo studies on geometrically confined skyrmions in nanodots: Stability and morphology under radial stresses. *Computational Materials Science*, 243, p.113137.

DOI : [10.1016/j.commatsci.2024.113137](https://doi.org/10.1016/j.commatsci.2024.113137)

[2] Ducharne, B., Deffo, Y.A.T., Sebald, G., Uchimoto, T., Gallais, C. and Ghibaudo, O., 2023. Low-frequency incremental permeability for the evaluation of deep carburization treatments: Theoretical understanding. *Journal of Magnetism and Magnetic Materials*, 586, p.171236.

DOI : [10.1016/j.jmmm.2023.171236](https://doi.org/10.1016/j.jmmm.2023.171236)

[3] Fagan, P., Zhang, S., Sebald, G., Uchimoto, T. and Ducharne, B., 2023. Barkhausen noise hysteresis cycle: Theoretical and experimental understanding. *Journal of Magnetism and Magnetic Materials*, 578, p.170810.

DOI : [10.1016/j.jmmm.2023.170810](https://doi.org/10.1016/j.jmmm.2023.170810)

[4] Ducharne, B., Deffo, Y.A.T., Zhang, S., Sebald, G., Lallart, M., Uchimoto, T., Gallais, C. and Ghibaudo, O., 2023. Carburization depth evaluation from magnetic nondestructive testing. *NDT & E International*, 137, p.102864.

DOI : [10.1016/j.ndteint.2023.102864](https://doi.org/10.1016/j.ndteint.2023.102864)

[5] Zhang, S., Ducharne, B., Sebald, G., Takeda, S. and Uchimoto, T., 2023. Magnetic indicators for evaluating plastic strains in electrical steel: Toward non-destructive assessment of the magnetic losses. *NDT & E International*, 134, p.102780.

DOI : [10.1016/j.ndteint.2022.102780](https://doi.org/10.1016/j.ndteint.2022.102780)

[6] Diguët, G., Ducharne, B., El Hog, S., Kato, F., Koibuchi, H., Uchimoto, T. and Diep, H.T., 2023. Monte Carlo studies of skyrmion stabilization under geometric confinement and uniaxial strain. *Journal of Magnetism and Magnetic Materials*, 579, p.170819.

DOI : [10.1016/j.jmmm.2023.170819](https://doi.org/10.1016/j.jmmm.2023.170819)